Supplemental: A Multi-Scale Model for Coupling Strands with Shear-Dependent Liquid

YUN (RAYMOND) FEI, Columbia University, USA
CHRISTOPHER BATTY, University of Waterloo, Canada
EITAN GRINSPUN and CHANGXI ZHENG, Columbia University, USA

This document presents supplemental material including an introduction to shear-dependent liquid, the derivation of 1D surface flow, the derivation of the derivatives of volume fraction, the relationship between compressible and incompressible mixtures, the connection between our additional inertia term on the strands with the prior work, the drag coefficient, the complementarity formulation of second-order Coulomb cone, the analytic form of Herschel-Bulkley plastic flow, the gradient and Hessian of the discrete curvatures used in discrete elastic rods, and the derivation of the Jacobian of shear force. Finally, we introduce our method for surface reconstruction and present the physical parameters used in this work.

CCS Concepts: • **Computing methodologies → Physical simulation**.

ACM Reference Format:

Yun (Raymond) Fei, Christopher Batty, Eitan Grinspun, and Changxi Zheng. 2019. Supplemental: A Multi-Scale Model for Coupling Strands with Shear-Dependent Liquid. *ACM Trans. Graph.* 38, 6, Article 1 (November 2019), 14 pages. https://doi.org/10.1145/3355089.3356532

S1 SHEAR-DEPENDENT LIQUID

In this section, we introduce background knowledge on shear-dependent liquid, which forms the basis of the simulation of the bulk liquid, the surface flow, their coupling, and the cohesion between strands. Below we summarize the theory behind our shear-dependent liquid, namely, the $\mathcal{J}_2$ liquid theory developed by Simo et al. [Simo 1988a]. Due to its simplicity and accuracy, this model is extensively used in prior work on simulating foams [Yue et al. 2015] and grains [Yue et al. 2018], and is employed as the constitutive model in this work.

The deformation gradient of a shear-dependent liquid is a second-order tensor defined over the liquid domain Ω, denoted as $\mathbf{F} = \frac{\partial \boldsymbol{\Psi}}{\partial \boldsymbol{x}} : \Omega \rightarrow \mathbb{R}^{d\times d}$, where $\boldsymbol{\Psi}$ is the deformation and d is the number of dimensions, i.e., $d = 2$ for 2D and $d = 3$ for 3D. Some shear-dependent liquids are compressible, and thus we need to consider their volume change, denoted as $J \equiv \det\mathbf{F}$, and we have [Bonet and Wood 1997]

$$\rho_{\mathrm{f}} = J^{-1}\rho_{\mathrm{f},0} \tag{S1}$$

where ρ_{f} is the liquid's (dynamic) mass density and $\rho_{\mathrm{f},0}$ is the mass density at rest.

It is convenient to decompose the deformation gradient $\mathbf{F}$ into parts associated to the elastic $\mathbf{F}^E$ and plastic $\mathbf{F}^P$ deformation via the decomposition [Bargteil et al. 2007; Irving et al. 2004; Jones et al. 2014; Simo and Hughes 2006; Wicke et al. 2010]

$$\mathbf{F} = \mathbf{F}^E\mathbf{F}^P. \tag{S2}$$

According to experimental observations [Bridgman 1949a,b], volume change is often reversible even when the liquid is under pressure up to $3\times10^{10}\mathrm{dyne/cm}^2$. In other words, the plastic deformation is usually volume preserving (or isochoric), i.e., $J^P = \det\mathbf{F}^P = 1$ and $J^E = \det\mathbf{F}^E = J$. Below we ignore the difference between J and J^E, and only deal with the volume change due to elastic deformation.

The elastic energy depends on the rotation-free *left Cauchy-Green tensor* $\mathbf{b} \equiv \mathbf{F}\mathbf{F}^T$ and, especially, its elastic part $\mathbf{b}^E \equiv \mathbf{F}^E\mathbf{F}^{E^T}$. The total energy density is then decomposed into

$$W = W_{\mathrm{v}}(J) + W_{\mathrm{s}}(\mathbf{b}^E) \tag{S3}$$

where W_{v} is the energy density resisting any volumetric change, and W_{s} is the shear-dependent energy density. Similar to prior work [Yue et al. 2015], we adopt a modified neo-Hookean model [Simo 1988a] and Rivlin's shear-dependent energy density [Rivlin 1948] for W_{v} and W_{s}, respectively. We have the following constitutive formulas

$$W_{\mathrm{v}}(J) = \frac{1}{2}\kappa\left(\frac{1}{2}(J^2-1) - \ln J\right), \tag{S4}$$

and

$$W_{\mathrm{s}}(\mathbf{b}^E) = \frac{1}{2}\mu\left(J^{E^{-\frac{2}{d}}}\mathrm{tr}\mathbf{b}^E - d\right). \tag{S5}$$

where κ and μ are the *bulk modulus* and the *shear modulus*.

The Kirchhoff Stress. After the energy densities are defined, the Kirchhoff stress tensor $\boldsymbol{\tau} \in \mathbb{R}^{d\times d}$ can be derived, as

$$\boldsymbol{\tau} \equiv \frac{\partial W}{\partial \mathbf{F}^E}\mathbf{F}^{E^T} = \frac{\kappa}{2}(J^2-1)\mathbf{I}_d + \mu J^{E^{-\frac{2}{d}}}\mathrm{dev}[\mathbf{b}^E], \tag{S6}$$

where $\mathbf{I}_d \in \mathbb{R}^{d\times d}$ is the d-dimension identity matrix, $\mathrm{dev}[\boldsymbol{x}] \equiv \boldsymbol{x} - \frac{tr[\boldsymbol{x}]}{d}\mathbf{I}_d$ is the deviatoric operator. In (S6), the first part is known as the *dilational Kirchhoff stress*, while the second part is the *shear*

Authors' addresses: Yun (Raymond) Fei, Columbia University, Computer Science, New York, NY, 10027, USA; Christopher Batty, University of Waterloo, Computer Science, Waterloo, ON, N2L 3G1, Canada; Eitan Grinspun; Changxi Zheng, Columbia University, Computer Science, New York, NY, 10027, USA.

0730-0301/2019/11-ART1 $15.00
https://doi.org/10.1145/3355089.3356532

Kirchhoff stress. The *Cauchy stress tensor* is then computed with $\boldsymbol{\sigma} \equiv \boldsymbol{\tau}/J$, which exactly matches (14) in the 3D case.

Pressure. We first compute the *dilational Cauchy stress* (which equals to the dilational Kirchhoff stress divided by J), following [Bonet and Wood 1997]:

$$\begin{aligned}\sigma_{\mathrm{v}} &= \frac{1}{J}\frac{\partial W_{\mathrm{v}}}{\partial \mathbf{F}^E}\mathbf{F}^{E^T} = \frac{1}{J}\frac{\partial W_{\mathrm{v}}}{\partial J^E}\frac{\partial J^E}{\partial \mathbf{F}^E}\mathbf{F}^{E^T} \\ &= \frac{1}{J}\frac{\partial W_{\mathrm{v}}}{\partial J^E}J^E\mathbf{F}^{E^{-T}}\mathbf{F}^{E^T} = \frac{1}{J}\frac{\partial W_{\mathrm{v}}}{\partial J^E}J^E\mathbf{I}_d \\ &= \frac{\partial W_{\mathrm{v}}}{\partial J^E}\mathbf{I}_d.\end{aligned} \tag{S7}$$

The negative value of this scalar applied on the d-dimensional identity matrix $\mathbf{I}_d$ is then defined as the *pressure* [Stomakhin et al. 2014], i.e.,

$$p \equiv -\frac{\partial W_{\mathrm{v}}}{\partial J^E}. \tag{S8}$$

Shear Kirchhoff Stress. The shear Kirchhoff stress is defined as the deviatoric part of $\boldsymbol{\tau}$. Since (S6) only contains diagonal terms in its first part, the shear Kirchhoff stress is equivalent to the second part of (S6), where

$$\mathbf{s} \equiv \mathrm{dev}[\boldsymbol{\tau}] = \mu J^{E^{-2/d}}\mathrm{dev}[\mathbf{b}^E]. \tag{S9}$$

Its scalar magnitude is

$$s = \|\mathbf{s}\| \tag{S10}$$

where $\|\cdot\|$ is the Frobenius norm. We will also make use of the normalized deviatoric stress tensor defined as $\hat{\mathbf{s}} \equiv \mathbf{s}/s$.

Plasticity. Once the shear stress is larger than some threshold, the liquid will yield to the shear stress and its elastic deformation will irreversibly convert into plastic deformation, i.e., there will be a plastic flow. In this work, we adopt the simple and efficient *von Mises yield condition* [Mises 1913] as the threshold for the onset of a plastic flow. This condition is written in the terms of the material-dependent yield stress τ_Y, as

$$\Phi(s) = s - \sqrt{\frac{2}{3}}\tau_Y \leq 0. \tag{S11}$$

For simplicity, we neglect any hardening or softening effects since they are not observable for the materials used in this work [Coussot 2017; Weaire and Hutzler 2001].

When the yield condition is violated, we compute the plastic flow according to the *yield excess* $\Phi(s)$ to estimate the excessive elastic strain that becomes the plastic strain. The temporal derivative of $\mathbf{b}^E$ is given as [Simo 1988a,b]

$$\frac{\mathrm{d}\mathbf{b}^E}{\mathrm{d}t} = \nabla\boldsymbol{u}_{\mathrm{f}}\mathbf{b}^E + \mathbf{b}^E\nabla\boldsymbol{u}_{\mathrm{f}}^T - \frac{2}{d}\mathrm{tr}[\mathbf{b}^E]\gamma(s)\hat{\mathbf{s}} \tag{S12}$$

where $\boldsymbol{u}_{\mathrm{f}} \in \mathbb{R}^{d\times 1}$ is the liquid velocity. The first two terms capture the change due to the flow field itself, while the last term captures the change due to plastic flow with flow rate denoted as γ (with physical unit s^{-1}).

In this work, we adopt the Herschel-Bulkley model [Herschel and Bulkley 1926] since it has been validated for a wide range of materials. The flow rate formula for γ is therefore

$$\gamma(s) = \max\left(0, \frac{\Phi(s)}{\eta}\right)^{1/n}, \tag{S13}$$

where η is the *flow consistency index* with physical unit $\mathrm{Ba}\cdot\mathrm{s}^n$ (or $\mathrm{Pa}\cdot\mathrm{s}^n$ in SI units), and n is the unitless *flow behavior index*. The liquid is pseudoplastic (shear-thinning) when $n < 1$, Newtonian when $n = 1$, and dilatant (shear-thickening) when $n > 1$.

The flow consistency index η indicates how slow the liquid would "forget" its elastic deformation. Liquid with a smaller η would become free from the elastic deformation more quickly. In the limit of $\eta \to 0$, any elastic deformation would immediately become plastic (Bingham plastics). If the yield stress is also zero, the liquid then becomes inviscid.

Remark: connection with a Newtonian liquid. By definition, a Newtonian liquid has a negligible elastic strain. We then rewrite the elastic Cauchy-Green strain as $\mathbf{b}^E = \mathbf{I}_d + \epsilon\frac{\mathrm{d}\mathbf{b}^E}{\mathrm{d}t}$ where $\epsilon \ll 1$ is a tiny positive perturbation variable. We also have $\tau_Y = 0$ and $n = 1$. (S12) then becomes

$$\begin{aligned}\epsilon\frac{\mathrm{d}^2\mathbf{b}^E}{\mathrm{d}t^2} &= \nabla\boldsymbol{u}_{\mathrm{f}}\left(\mathbf{I}_d + \epsilon\frac{\mathrm{d}\mathbf{b}^E}{\mathrm{d}t}\right) + \left(\mathbf{I}_d + \epsilon\frac{\mathrm{d}\mathbf{b}^E}{\mathrm{d}t}\right)\nabla\boldsymbol{u}_{\mathrm{f}}^T \\ &\quad - 2\left(1 + \frac{\epsilon}{d}\mathrm{tr}\left[\frac{\mathrm{d}\mathbf{b}^E}{\mathrm{d}t}\right]\right)\mathbf{s}\eta^{-1}\end{aligned} \tag{S14}$$

After some algebraic manipulation, we have a shear stress $\mathbf{s}$ equivalent to the viscous tensor for the Newtonian fluid, which proves that the flow consistency index plays the same role as the viscosity coefficient in a Newtonian liquid

$$\mathbf{s} = \frac{\eta}{2}\left(\nabla\boldsymbol{u}_{\mathrm{f}} + \nabla\boldsymbol{u}_{\mathrm{f}}^T\right) + O(\epsilon). \tag{S15}$$

Hence, as $\tau_Y = 0$ and $n = 1$, the model presented in this section degenerates to the viscous Newtonian fluid model.

S2 DERIVATION OF THE 1D SURFACE FLOW

In §3.1 of the main paper, we have taken the plane-strain conditions, where we can safely ignore the velocity in the angular direction around the strand. Thus we can derive a 1D surface flow model from the 2D theory of shear-dependent liquid introduced in §S1. For legibility in the following discussion we use the label of the axis to represent the corresponding row or column in the subscript of a strain or stress tensor, i.e., x for the first row or column, y for the second row or column.

Parameter Scaling. We denote the height of the flow as h, and we have the velocity in the y-axis, i.e., radial axis, denoted as $v = \frac{\partial h}{\partial y}$. The velocity of the 2D flow is then denoted as $\boldsymbol{u}_{\mathrm{f}} \equiv (u_\tau, v)$. From our assumptions (see §3.1), the surface flow is thin in height, where we can define a scaling parameter $0 < \epsilon \equiv \frac{r}{L} \ll 1$, and we define

$$h \equiv \epsilon H, y \equiv \epsilon Y, v \equiv \epsilon V, b^E_{xy} \equiv \epsilon B^E_{xy}. \tag{S16}$$

Additionally, we deduce that $\partial/\partial y = \epsilon^{-1}\partial/\partial Y$.

To expand a scalar to a matrix, we adopt the notation below:

$$[*]_{\mathrm{e}} \equiv [*, 0; 0, 0] \in \mathbb{R}^{2\times 2}, [*]_{\mathrm{s}} \equiv [0, *; *, 0] \in \mathbb{R}^{2\times 2}. \tag{S17}$$

Reduced Cauchy-Green Strain. The 2D left Cauchy-Green elastic strain tensor $\mathbf{b}^E$ can then be written as

$$\mathbf{b}^E = [c_\tau^E]_{\mathrm{e}} + b_{yy}^E \mathbf{I}_2 + \epsilon [B_{xy}^E]_{\mathrm{s}} \tag{S18}$$

where $c_\tau^E \equiv b_{xx}^E - b_{yy}^E$ is called the *reduced left Cauchy-Green strain*. In the following derivation, we will discover its temporal derivative, which is used to evolve the liquid's elastic and plastic deformation, and the momentum equation, which uses c_τ to compute shear stress.

By applying the deviatoric operator to both sides of (S18), we have

$$\mathrm{dev}[\mathbf{b}^E] = \mathrm{dev}[[c_\tau^E]_{\mathrm{e}}] + \epsilon [B_{xy}^E]_{\mathrm{s}} \tag{S19}$$

and according to the definition of shear stress (refer to §S1), we can rewrite the norm of shear stress as

$$s_\tau = \mu J^{E^{-1}} \|\mathrm{dev}[\mathbf{b}^E]\| = \mu J^{E^{-1}} \sqrt{\frac{1}{2}\left(c_\tau^E\right)^2 + 2\epsilon^2 {B_{xy}^E}^2}. \tag{S20}$$

The derivative of c_τ^E is then computed as

$$\dot{c}_\tau^E = \dot{b}_{xx}^E - \dot{b}_{yy}^E \tag{S21}$$

$$= 2\left(\frac{\partial u_\tau}{\partial x} - \frac{\sqrt{2} c_\tau^E \gamma(s_\tau)}{\sqrt{{c_\tau^E}^2 + 4\epsilon^2 {B_{xy}^E}^2}}\right)\left(c_\tau^E + b_{yy}^E\right) \tag{S22}$$

$$+ 2\left(\frac{\partial u_\tau}{\partial y} - \frac{\partial v}{\partial x}\right)\epsilon B_{xy}^E - 2\frac{\partial v}{\partial y} b_{yy}^E. \tag{S23}$$

From assumption (1) in §3.1, we only consider the *average* longitudinal velocity u_τ across its depth, i.e., $\partial u_\tau / \partial y = 0$. With the scaling proposed in (S16), we can approximate $\dot{c}_\tau^E$ by neglecting the terms multiplied with ϵ^2, as follows:

$$\dot{c}_\tau^E = 2\left(\frac{\partial u_\tau}{\partial x} - \sqrt{2}\gamma(s)\mathrm{sgn}(c_\tau^E)\right)\left(c_\tau^E + b_{yy}^E\right) - 2\frac{\partial v}{\partial y} b_{yy}^E + O(\epsilon^2) \tag{S24}$$

We then use the incompressibility condition proposed in assumption (2) in §3.1,

$$\frac{\partial u_\tau}{\partial x} + \frac{\partial v}{\partial y} = 0, \det[\mathbf{b}^E] = 1, \tag{S25}$$

to eliminate v and b_{yy}^E. For the latter we have

$$\det[\mathbf{b}^E] = {b_{yy}^E}^2 + c_\tau^E b_{yy}^E + O(\epsilon^2) = 1. \tag{S26}$$

Since $b_{yy}^E \geq 0$, we then have

$$b_{yy}^E = \frac{\sqrt{{c_\tau^E}^2 + 4 - O(\epsilon^2)} - c_\tau^E}{2} \tag{S27}$$

By substitution of (S25), (S27) into (S24), and with the ϵ^2 terms neglected, we have the temporal derivative of c_τ^E in the same form as (3).

Similar to the case in the 3D model (§S1), as $\tau_Y = 0$ and $n = 1$, the magnitude of shear stress s_τ is proportional to the viscosity η and the reduced elastic strain c_τ^E, i.e., $s_\tau = \sqrt{2}\eta c_\tau^E$, which indicates that the reduced model degenerates to a (reduced) viscous Newtonian fluid model.

Shear Stress. After performing a decomposition to the 2D deviatoric Kirchhoff stress $\mathrm{dev}[\boldsymbol{\tau}]$, we have

$$\mathrm{dev}[\boldsymbol{\tau}] = \mathrm{dev}[[\tau_{xx} - \tau_{yy}]_{\mathrm{e}}] + [\tau_{xy}]_{\mathrm{s}}. \tag{S28}$$

From (S6) we then have

$$\mathrm{dev}[\boldsymbol{\tau}] = \mu \mathrm{dev}[[c_\tau^E]_{\mathrm{e}}] + \mu\epsilon [B_{xy}^E]_{\mathrm{s}} \approx \mu \mathrm{dev}[[c_\tau^E]_{\mathrm{e}}]. \tag{S29}$$

The 2D Cauchy stress tensor is therefore computed as (using the incompressibility assumption $J = 1$)

$$\boldsymbol{\sigma}_{2D} = \mu \mathrm{dev}[[c_\tau^E]_{\mathrm{e}}] - p\mathbf{I}_2. \tag{S30}$$

Since our flow is symmetric around the strand centerline, with the plane strain conditions the 3D stress tensor $\boldsymbol{\sigma}$ can be specified with this 2D stress tensor, where we have

$$\boldsymbol{\sigma} = [\boldsymbol{\sigma}_{2D,xx}, \boldsymbol{\sigma}_{2D,xy}, 0; \boldsymbol{\sigma}_{2D,xy}, \boldsymbol{\sigma}_{2D,yy}, 0; 0, 0, (\boldsymbol{\sigma}_{2D,xx} + \boldsymbol{\sigma}_{2D,yy})/2r]. \tag{S31}$$

which will be used in the following derivation for a 1D reduced momentum equation.

Variational form of the Momentum Equation. In the following we derive the 1D reduced momentum equation from the 3D Navier-Stokes momentum equation, which reads

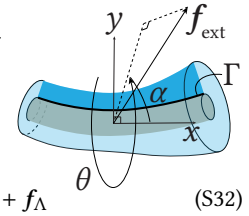

$$\rho_{\mathrm{f}} \frac{\mathrm{D}\boldsymbol{u}_{\mathrm{f}}}{\mathrm{D}t} - \nabla \cdot \boldsymbol{\sigma} = \boldsymbol{f}_{\mathrm{ext}} + \boldsymbol{f}_\Lambda \tag{S32}$$

where $\boldsymbol{f}_\Lambda$ is the frictional force on the bottom of the flow; $\boldsymbol{f}_{\mathrm{ext}}$ is the external body force such as gravity and inertial force; and $\boldsymbol{\sigma}$ is the Cauchy stress tensor. We denote the interface between the reduced surface flow and the strand as Γ, and define a trial function $\boldsymbol{\Phi} \equiv (\Phi_x, \Phi_y, \Phi_\theta)$ that is a vector defined in the cylindrical coordinate whose x-axis is aligned with the longitudinal direction of the strand. The weak formulation of (S32) can be written as

$$\int_0^{2\pi}\int_r^{r+h_\tau}\int_\Gamma \left[\rho_{\mathrm{f}}\left(\frac{\partial \boldsymbol{u}_{\mathrm{f}}}{\partial t} + \boldsymbol{u}_{\mathrm{f}} \cdot \nabla \boldsymbol{u}_{\mathrm{f}}\right) \cdot \boldsymbol{\Phi} + \boldsymbol{\sigma} : \mathbf{D}(\boldsymbol{\Phi})\right] y \mathrm{d}x\mathrm{d}y\mathrm{d}\theta$$
$$+ \int_0^{2\pi}\int_\Gamma \sigma_{yy}\Phi_y r \mathrm{d}x\mathrm{d}y\mathrm{d}\theta = \int_0^{2\pi}\int_r^{r+h_\tau}\int_\Gamma (\boldsymbol{f}_\Lambda + \boldsymbol{f}_{\mathrm{ext}}) \cdot \boldsymbol{\Phi} y \mathrm{d}x\mathrm{d}y\mathrm{d}\theta \tag{S33}$$

where σ_{yy} is the pressure applied to the flow by the strand surface Γ, $\mathbf{D}$ is the rate of deformation tensor, i.e., $\mathbf{D}(\boldsymbol{\Phi}) \equiv (1/2)\left(\nabla\boldsymbol{\Phi} + \nabla^T\boldsymbol{\Phi}\right)$. In the following derivation we will use two deductions based on the assumptions made in §3.1: 1) due to the symmetry of the flow, we have $\boldsymbol{u}_{\mathrm{f}} = (u_\tau, v, 0)$; and 2) due to the incompressibility of the flow, we have

$$\frac{\partial u_\tau}{\partial x} + \frac{\partial v}{\partial y} = 0. \tag{S34}$$

Integrating the above equation over the y-axis from Γ to the free surface, and using the fact that $v|_\Gamma = 0$, i.e., the flow cannot penetrate the strand surface, we have

$$v = -y\frac{\partial u_\tau}{\partial x}. \tag{S35}$$

Pressure of the Reduced Surface Flow. To derive the pressure σ_{yy}, we first choose a trial function by setting $\Phi_x = 0$ and $\Phi_\theta = 0$, i.e., only allowing $\Phi_y \neq 0$. With (S29), (S30), and (S31) substituted into (S33), and with the variables replaced with our scaled ones proposed in (S16), we have

$$\epsilon^3 \int_0^{2\pi} \int_r^{r+\epsilon H} \int_\Gamma \left[-H^3 Y^3 \rho_\mathrm{f} \left(\frac{\partial^2 u_\tau}{\partial t \partial x} + \boldsymbol{u}_\tau \frac{\partial^2 u_\tau}{\partial x^2} - \left(\frac{\partial u_\tau}{\partial x} \right)^2 \right) \Phi_y + \mu H^2 Y^2 B^\mathrm{E}_{xy} \frac{\partial \Phi_y}{\partial x} \right] \mathrm{d}x\mathrm{d}Y\mathrm{d}\theta + \epsilon \int_0^{2\pi} \int_\Gamma \sigma_{yy} \Phi_y r H \mathrm{d}x\mathrm{d}Y\mathrm{d}\theta = \epsilon^2 \int_0^{2\pi} \int_r^{r+h_\tau} \int_\Gamma \|\boldsymbol{f}_\mathrm{ext}\| \sin\alpha \cos\theta H^2 Y \mathrm{d}x\mathrm{d}Y\mathrm{d}\theta \tag{S36}$$

where α is the angle between the direction (in Euclidian space) of x-axis of the cylindrical coordinate and the direction of external force projected onto the xy-plane.

The right-hand side of (S36) is zero since the external force perpendicular to the strand cancels after being integrated over $\mathrm{d}\theta$. By dividing both sides by ϵ and discarding the remaining high-order terms multiplied with ϵ^2, we have

$$\int_0^{2\pi} \int_\Gamma \sigma_{yy} \Phi_y r H \mathrm{d}x\mathrm{d}Y\mathrm{d}\theta = 0, \tag{S37}$$

for arbitrary Φ_y, which simply indicates

$$\sigma_{yy} = 0. \tag{S38}$$

Momentum Equation of Reduced Surface Flow. To derive the reduced momentum equation about u_τ, we choose another trial function by setting $\boldsymbol{\Phi} = (\Phi_x, -y\frac{\partial \Phi_x}{\partial x}, 0)$ — the middle term is set according to (S35). After the variables in (S33) are replaced with our scaled ones, and (S38) is used, we have

$$\epsilon^2 \int_0^{2\pi} \int_r^{r+\epsilon H} \int_\Gamma H^2 Y \left[\rho_\mathrm{f} \left(\frac{\partial u_\tau}{\partial t} + u_\tau \frac{\partial u_\tau}{\partial x} \right) \Phi_x + \mu c_\tau^E \frac{\partial \Phi_x}{\partial x} \right] + \epsilon^4 \int_0^{2\pi} \int_r^{r+\epsilon H} \int_\Gamma \left[H^4 Y^4 \rho_\mathrm{f} \left(\frac{\partial^2 u_\tau}{\partial t \partial x} + \boldsymbol{u}_\tau \frac{\partial^2 u_\tau}{\partial x^2} - \left(\frac{\partial u_\tau}{\partial x} \right)^2 \right) \frac{\partial \Phi_x}{\partial x} + \mu H^3 Y^3 B^\mathrm{E}_{xy} \frac{\partial^2 \Phi_x}{\partial x^2} \right] \mathrm{d}x\mathrm{d}Y\mathrm{d}\theta = \epsilon^2 \int_0^{2\pi} \int_r^{r+\epsilon H} \int_\Gamma H^2 Y \left[\left(\|\boldsymbol{f}_\mathrm{ext}\| \cos\alpha + f_\Lambda \right) \Phi_x - \epsilon \|\boldsymbol{f}_\mathrm{ext}\| \sin\alpha \cos\theta H Y \frac{\partial \Phi_x}{\partial x} \right] \mathrm{d}x\mathrm{d}Y\mathrm{d}\theta \tag{S39}$$

where f_Λ is the magnitude of frictional force. The last term on the right hand side of (S39) is again an external force perpendicular to the strand, which will be canceled after being integrated over $\mathrm{d}\theta$. We then divide both sides with ϵ^2 and discard the remaining high-order terms containing ϵ^2, which gives us

$$\int_0^{2\pi} \int_r^{r+\epsilon H} \int_\Gamma \left[\rho_\mathrm{f} \left(\frac{\partial u_\tau}{\partial t} + u_\tau \frac{\partial u_\tau}{\partial x} \right) \Phi_x + \mu c_\tau^E \frac{\partial \Phi_x}{\partial x} \right] H^2 Y \mathrm{d}x\mathrm{d}Y\mathrm{d}\theta = \int_0^{2\pi} \int_r^{r+\epsilon H} \int_\Gamma \left(\|\boldsymbol{f}_\mathrm{ext}\| \cos\alpha + f_\Lambda \right) \Phi_x H^2 Y \mathrm{d}x\mathrm{d}Y\mathrm{d}\theta. \tag{S40}$$

Furthermore, the term $\int_0^{2\pi} \int_r^{r+\epsilon H} H^2 Y dY d\theta = \pi h_\tau (h_\tau + 2r)$ is the *cross-sectional area* of the flow, and can be integrated individually since the other terms are independent of Y and θ. After reordering the multiple integrations in (S40), we have

$$\int_\Gamma \left[\rho_\mathrm{f} \left(\frac{\partial u_\tau}{\partial t} + u_\tau \frac{\partial u_\tau}{\partial x} \right) \Phi_x + \mu c_\tau^E \frac{\partial \Phi_x}{\partial x} \right] \int_0^{2\pi} \int_r^{r+\epsilon H} H^2 Y \mathrm{d}Y\mathrm{d}\theta\mathrm{d}x = \int_\Gamma \left(\|\boldsymbol{f}_\mathrm{ext}\| \cos\alpha + f_\Lambda \right) \Phi_x \int_0^{2\pi} \int_r^{r+\epsilon H} H^2 Y \mathrm{d}Y\mathrm{d}\theta\mathrm{d}x. \tag{S41}$$

For brevity, we denote the cross section as A_τ below. We then replace the variables in (S41) with the non-scaled version, which reads

$$\int_\Gamma \rho_\mathrm{f} A_\tau \left(\frac{\partial u_\tau}{\partial t} + u_\tau \frac{\partial u_\tau}{\partial x} \right) \Phi_x + \mu A_\tau c_\tau^E \frac{\partial \Phi_x}{\partial x} = \int_\Gamma A_\tau \left(\|\boldsymbol{f}_\mathrm{ext}\| \cos\alpha + f_\Lambda \right) \Phi_x \mathrm{d}x, \tag{S42}$$

for arbitrary Φ_x. The corresponding momentum equation is then

$$\rho_\mathrm{f} A_\tau \left(\frac{\partial u_\tau}{\partial t} + u_\tau \frac{\partial u_\tau}{\partial x} \right) - \mu \frac{\partial A_\tau c_\tau^E}{\partial x} = A_\tau \left(f_{\mathrm{ext},x} + f_\Lambda \right), \tag{S43}$$

where $f_{\mathrm{ext},x} \equiv \|\boldsymbol{f}_\mathrm{ext}\| \cos\alpha$. Substituting f_Λ with the friction model proposed in section 3.1, we have exactly the form of (2).

S3 DERIVATIVES OF VOLUME FRACTION

We begin our derivation from (10). By taking its spatial derivative, we have (with the location parameter $\boldsymbol{x}$ dropped for brevity)

$$\nabla \epsilon_\mathrm{s} = \frac{\partial \epsilon_\mathrm{s}}{\partial \boldsymbol{x}} = \frac{\sum_i V_i \nabla w_{R,i}}{V^*}. \tag{S44}$$

Similarly we take the divergence of (11), where we have

$$\nabla \cdot (\epsilon_\mathrm{s} \bar{\boldsymbol{u}}_\mathrm{s}) = \frac{\sum_i V_i \nabla \cdot (\boldsymbol{u}_{\mathrm{s},i} w_{R,i})}{V^*}. \tag{S45}$$

Since we have assumed that each rod element is incompressible, we have $\nabla \cdot \boldsymbol{u}_{\mathrm{s},i} = 0$, and thus the equation above can be rewritten as

$$\nabla \cdot (\epsilon_\mathrm{s} \bar{\boldsymbol{u}}_\mathrm{s}) = \frac{\sum_i V_i \boldsymbol{u}_{\mathrm{s},i} \cdot \nabla w_{R,i}}{V^*}. \tag{S46}$$

In mixture theory [Anderson and Jackson 1967], the continuity equation for a solid with constant mass density reads

$$\frac{\partial \epsilon_\mathrm{s}}{\partial t} + \nabla \cdot (\epsilon_\mathrm{s} \bar{\boldsymbol{u}}_\mathrm{s}) = 0. \tag{S47}$$

Using (S47), the material derivative of the solid volume fraction ϵ_s advected along with liquid velocity $\boldsymbol{u}_\mathrm{f}$ is then derived as follows:

$$\frac{\mathrm{D}_{\boldsymbol{u}_\mathrm{f}} \epsilon_\mathrm{s}}{\mathrm{D}t} \equiv \frac{\partial \epsilon_\mathrm{s}}{\partial t} + \boldsymbol{u}_\mathrm{f} \cdot \nabla \epsilon_\mathrm{s} \tag{S48}$$

$$= \boldsymbol{u}_\mathrm{f} \cdot \nabla \epsilon_\mathrm{s} - \nabla \cdot (\epsilon_\mathrm{s} \bar{\boldsymbol{u}}_\mathrm{s}). \tag{S49}$$

By replacing the terms defined in (S44) and (S46), we have

$$\frac{\mathrm{D}_{\boldsymbol{u}_\mathrm{f}} \epsilon_\mathrm{s}}{\mathrm{D}t} = \boldsymbol{u}_\mathrm{f} \cdot \frac{\sum_i V_i \nabla w_{R,i}}{V^*} - \frac{\sum_i V_i \boldsymbol{u}_{\mathrm{s},i} \cdot \nabla w_{R,i}}{V^*} \tag{S50}$$

$$= \frac{\sum_i V_i (\boldsymbol{u}_\mathrm{f} - \boldsymbol{u}_{\mathrm{s},i}) \cdot \nabla w_{R,i}}{V^*}. \tag{S51}$$

which matches (12).

S4 RELATIONSHIP WITH INCOMPRESSIBLE MIXTURES

The derivation in this section is not limited to a specific constitutive model. For an arbitrary non-zero dilational potential energy whose second-order derivative is denoted as $\kappa g(J^E)$ below, we may rewrite (18a) into the following form:

$$\frac{\mathrm{D}_{\boldsymbol{u}_\mathrm{f}} p}{\mathrm{D}t} = -\kappa g(J^E)\left(\epsilon_\mathrm{f}^{-1}\frac{\mathrm{D}_{\boldsymbol{u}_\mathrm{f}}\epsilon_\mathrm{f}}{\mathrm{D}t} + \nabla\cdot\boldsymbol{u}_\mathrm{f} - \frac{1}{J^P}\frac{\mathrm{D}_{\boldsymbol{u}_\mathrm{f}} J^P}{\mathrm{D}t}\right). \tag{S52}$$

For an incompressible mixture we have the liquid material stiffness $\kappa \to \infty$ and $J^P = 1$. By dividing both sides by κ and taking the infinite limit of κ, we have

$$\lim_{\kappa\to\infty}\left(\kappa^{-1}\frac{\mathrm{D}_{\boldsymbol{u}_\mathrm{f}} p}{\mathrm{D}t}\right) = 0 = -g(J^E)\left(\epsilon_\mathrm{f}^{-1}\frac{\mathrm{D}_{\boldsymbol{u}_\mathrm{f}}\epsilon_\mathrm{f}}{\mathrm{D}t} + \nabla\cdot\boldsymbol{u}_\mathrm{f}\right) \tag{S53}$$

or simply (since g is non-zero)

$$\frac{\mathrm{D}_{\boldsymbol{u}_\mathrm{f}}\epsilon_\mathrm{f}}{\mathrm{D}t} + \epsilon_\mathrm{f}\nabla\cdot\boldsymbol{u}_\mathrm{f} = 0, \tag{S54}$$

which can be rewritten by expanding the material derivative $\mathrm{D}_{\boldsymbol{u}_\mathrm{f}}\epsilon_\mathrm{f}/\mathrm{D}t$, as

$$\frac{\partial\epsilon_\mathrm{f}}{\partial t} + \nabla\cdot(\epsilon_\mathrm{f}\boldsymbol{u}_\mathrm{f}) = 0. \tag{S55}$$

This is exactly the continuity equation for liquid in a mixture with constant mass density (see e.g., [Anderson and Jackson 1967]). After (S47) is added with (S55), we obtain the equation for incompressible mixtures that is used in prior work [Fei et al. 2018; Gao et al. 2018]:

$$\nabla\cdot(\epsilon_\mathrm{f}\boldsymbol{u}_\mathrm{f} + \epsilon_\mathrm{s}\boldsymbol{u}_\mathrm{s}) = 0. \tag{S56}$$

S5 EQUIVALENCE OF THE ADDITIONAL INERTIA TO THE PRIOR WORK

In this section we prove that the momentum transfer proposed by Fei et al. [2017] is equivalent to the (rightmost) additional inertia term in (9), when both are integrated explicitly. We begin from the momentum transfer equation. With our notations, it reads

$$\frac{\partial}{\partial t}(\boldsymbol{u}_\mathrm{s}A_\tau) + \frac{\partial}{\partial x}(\boldsymbol{u}_\mathrm{s}A_\tau u_\tau) = 0, \tag{S57}$$

which can be re-written through the product rule, as

$$A_\tau\left(\frac{\partial\boldsymbol{u}_\mathrm{s}}{\partial t} + u_\tau\frac{\partial\boldsymbol{u}_\mathrm{s}}{\partial x}\right) + \boldsymbol{u}_\mathrm{s}\left(\frac{\partial A_\tau}{\partial t} + \frac{\partial}{\partial x}(A_\tau u_\tau)\right) = 0. \tag{S58}$$

According to the mass conservation (7) of the surface flow, the second term multiplied on $\boldsymbol{u}_\mathrm{s}$ is zero, i.e.,

$$\frac{\partial A_\tau}{\partial t} + \frac{\partial}{\partial x}(A_\tau u_\tau) = 0 \tag{S59}$$

Therefore, as long as the strand is wet, i.e., $A_\tau > 0$, we have

$$\frac{\partial\boldsymbol{u}_\mathrm{s}}{\partial t} = -u_\tau\nabla\boldsymbol{u}_\mathrm{s}. \tag{S60}$$

Fei et al. [2017] firstly solve the momentum transfer (S57), which, according to the derivation above, is equivalent to solving (S60). With an explicit integration of (S60), we have

$$\tilde{\boldsymbol{u}}_\mathrm{s} \leftarrow \hat{\boldsymbol{u}}_\mathrm{s} - hu_\tau\nabla\boldsymbol{u}_\mathrm{s}, \tag{S61}$$

where $\hat{\boldsymbol{u}}_\mathrm{s}$ and $\tilde{\boldsymbol{u}}_\mathrm{s}$ denote the strands' velocities before and after the momentum transfer is done. Fei et al. [2017] then modify the strands' velocity, as

$$\boldsymbol{u}_\mathrm{s} \leftarrow (m_\mathrm{s} + m_\tau)^{-1}(m_\mathrm{s}\hat{\boldsymbol{u}}_\mathrm{s} + m_\tau\tilde{\boldsymbol{u}}_\mathrm{s}), \tag{S62}$$

where m_s and m_τ are the rod and surface flow mass, respectively. By substituting (S61) into (S62) and rearranging the terms, we have

$$(m_\mathrm{s} + m_\tau)\boldsymbol{u}_\mathrm{s} = (m_\mathrm{s} + m_\tau)\hat{\boldsymbol{u}}_\mathrm{s} - hm_\tau u_\tau\nabla\boldsymbol{u}_\mathrm{s}, \tag{S63}$$

which is exactly the explicit discretization of the strands' momentum equation (9) with all the other forces on its right hand side integrated into $\hat{\boldsymbol{u}}_\mathrm{s}$.

S6 DRAG COEFFICIENT

The drag coefficient for rod element i has the following form [Rajitha et al. 2006]:

$$\begin{aligned} C_{\mathrm{d},i} = C_{\mathrm{d}0,i} + \frac{A_{\mathrm{c},i}}{A_{\perp,i}}C_{\mathrm{d}\infty}(C_{\mathrm{d}0,i})^{2\beta}k\left[\frac{6Xb}{6Xb + C_{\mathrm{d}0,i}}\right]^\beta \\ + C_{\mathrm{d}\infty}\left[\frac{6Xb}{6Xb + 128C_{\mathrm{d}0,i}}\right], \end{aligned} \tag{S64}$$

where $A_{\mathrm{c},i}$ is the surface area of the i-th element, $A_{\perp,i}$ is the area of the i-th discrete element projected in the direction of relative velocity, and

$$C_{\mathrm{d}0,i} \equiv \frac{24X}{\mathrm{Re}_{\mathrm{p},i}}, \tag{S65a}$$

$$C_{\mathrm{d}\infty} \equiv 0.44, \tag{S65b}$$

$$\alpha \equiv \frac{3}{n^2 + n + 1}, \tag{S65c}$$

$$X \equiv 6^{(n-1)/2}\alpha^{n+1}, \tag{S65d}$$

$$b \equiv \exp\left[3(\alpha - \ln 6)\right], \tag{S65e}$$

$$k \equiv \frac{3-\alpha}{6\alpha}\exp\left(\frac{3-\alpha}{2\alpha}\ln 3\right), \tag{S65f}$$

$$\beta \equiv \frac{11}{48}\sqrt{6}\left[1 - \exp\left[\left(\frac{3-\alpha}{2\alpha}\right)^2\ln\left(\frac{\sqrt{6}-1}{\sqrt{6}}\right)\right]\right]. \tag{S65g}$$

where $\mathrm{Re}_{\mathrm{p},i}$ is the *particle Reynolds number* (see below) of the i-th element, and n is the flow behavior index.

The particle Reynolds number for Herschel-Bulkley liquid. The drag coefficient proposed in (S64) was originally developed for power-law fluids. Nevertheless, Atapattu et al. [1995] showed that a drag coefficient for a power-law fluid can also be generalized to Herschel-Bulkley liquid by adopting a modified particle Reynolds number. Using the von Mises yield condition (S11), the particle Reynolds number for the i-th rod element reads [Atapattu et al. 1995; Di Felice 1994]:

$$\mathrm{Re}_{\mathrm{p},i} \equiv \frac{\epsilon_\mathrm{f}\rho_\mathrm{f}d_{\mathrm{p},i}^n\|\boldsymbol{u}_\mathrm{f} - \boldsymbol{u}_{\mathrm{s},i}\|^2}{\eta\|\boldsymbol{u}_\mathrm{f} - \boldsymbol{u}_{\mathrm{s},i}\|^n + \sqrt{\frac{2}{3}}\tau_Y d_{\mathrm{p},i}^n} \tag{S66}$$

where $d_{\mathrm{p},i}$ is the diameter of a circle that has area equivalent to $A_{\perp,i}$, i.e., $d_{\mathrm{p},i} = 2\sqrt{A_{\perp,i}/\pi}$.

We plot the drag coefficient over its different parameters in Fig. S1, where we can observe that the drag coefficient increases over the

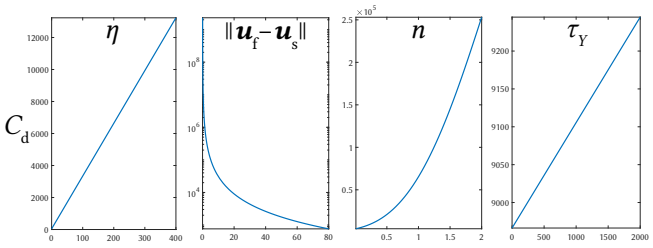

Fig. S1. **Drag coefficient over its different parameters.** Data is acquired through varying one parameter and fixing the others with the parameters of shaving cream.

flow consistency index (or viscosity) η, the yield stress τ_Y, the flow behavior index n, and decreases over the relative velocity between liquid and strand element.

Degeneration to a Drag Coefficient in Newtonian liquid. In a Newtonian liquid, the flow behavior index $n = 1$. Then in the equations above, $X = 1$, $\alpha = 1$, and $k = 1$, where (S64) is precisely consistent with the drag coefficient for irregular particles in Newtonian liquid [Mauret and Renaud 1997].

Sanity Check through Dimensional Analysis. Dimensional analysis provides a useful sanity check. As mentioned in §S1, the flow consistency index has physical units of $\mathrm{Ba}\cdot\mathrm{s}^n$, and the yield condition τ_Y has physical units of pressure (Ba). The divisor in (S66) then has physical units $\mathrm{Ba}\cdot\mathrm{cm}^n$, or $\mathrm{g}\cdot\mathrm{cm}^{n-1}\cdot\mathrm{s}^{-2}$, which exactly cancels with the physical units of the dividend. Hence Re_p is indeed a unitless number. Obviously all the parameters in (S65) are unitless, thence C_d is unitless. Furthermore, χ defined in (20) is unitless. Therefore $\boldsymbol{f}_{\mathrm{drag,s}}$ has physical units of $\mathrm{g}\cdot\mathrm{cm}\cdot\mathrm{s}^{-2}$, or a dyne, which is precisely the units of a force. In (21), the weighted sum also has units of a force. With the divisor V^* applied, $\boldsymbol{f}_{\mathrm{drag,f}}$ has the units of a *force density*, which matches exactly the units of both sides of (13).

S7 COMPLEMENTARITY FORMULATION OF THE SOCCP

After adopting the change of variables proposed by De Saxcé and Feng [1998] and Daviet et al. [2011], we have the following complementarity formulation of a self-dual cone $\mathbb{K} \equiv \mathbb{K}_{\mu=1}$:

$$\mathbb{K} \ni \hat{\boldsymbol{v}} \perp \hat{\boldsymbol{r}} \in \mathbb{K} \tag{S67}$$

where

$$\hat{\boldsymbol{r}} \equiv [\mu r_{\mathrm{s,N}}; \boldsymbol{r}_{\mathrm{s,T}}], \hat{\boldsymbol{v}} \equiv \overline{m}_\mathrm{s}[\tilde{v}_\mathrm{N}; \mu\tilde{\boldsymbol{v}}_\mathrm{T}], \tag{S68}$$

and

$$\tilde{\boldsymbol{v}} \equiv \boldsymbol{v} + \mu\|\boldsymbol{v}_\mathrm{T}\|\boldsymbol{n}. \tag{S69}$$

In (S68), the mass $\overline{m}_\mathrm{s} = (m_{s,1} + m_{s,2})/2$ is the averaged mass of the elements in contact, which scales the velocity so that $\overline{m}_\mathrm{s}\hat{\boldsymbol{v}}$ has the same physical units as $\hat{\boldsymbol{r}}$.

Then solving for $\hat{\boldsymbol{r}}$ in (S67) can be converted into a root-finding problem [Daviet et al. 2011; Fukushima et al. 2002]

$$\mathbb{K} \ni \boldsymbol{x} \perp \boldsymbol{y} \in \mathbb{K} \Leftrightarrow \boldsymbol{f}^{\mathrm{MFB}}(x, y) = \boldsymbol{0} \tag{S70}$$

where

$$\boldsymbol{f}^{\mathrm{MFB}}(\boldsymbol{x}, \boldsymbol{y}) \equiv \boldsymbol{x} \circ \boldsymbol{y} - (\boldsymbol{x} \circ \boldsymbol{x} + \boldsymbol{y} \circ \boldsymbol{y})^{\frac{1}{2}} \tag{S71}$$

is known as the *modified Fischer-Burmeister* (MFB) function, and the operator $\circ$ is the Jordan product defined as

$$\boldsymbol{x} \circ \boldsymbol{y} \equiv [\boldsymbol{x} \cdot \boldsymbol{y}; x_\mathrm{N}\boldsymbol{y}_\mathrm{T} + y_\mathrm{N}\boldsymbol{x}_\mathrm{T}]. \tag{S72}$$

S8 THE COHESIVE FORCE

In this work, the capillary part of the cohesive force follows Fei et al. [2017], which gives it as the negative gradient of the capillary potential. With our notations, it reads

$$f_\mathrm{N}(g) = \int_\Psi \frac{\mathrm{d}}{\mathrm{d}g}\mathrm{d}E_\mathrm{s}(s), \tag{S73}$$

where Ψ is the domain (in length) over which the surface flows on two rod elements are in contact. The cross-sectional surface potential is expressed as

$$\mathrm{d}E_\mathrm{s}(s) = \sigma\left[l_\mathrm{A}(s) + \cos\theta_1 l_{\mathrm{S1}}(s) + \cos\theta_2 l_{\mathrm{S2}}(s)\right]\mathrm{d}s \tag{S74}$$

where l_A is the length of the liquid-air interface given by

$$l_\mathrm{A}(s) = R(s)[\pi - (\theta_1 + \theta_2 + \alpha_1(s) + \alpha_2(s))]. \tag{S75}$$

Here, l_{S1} and l_{S2} are the arc lengths of the two rod-air boundaries with θ_1 and θ_2 as their contact angles, which are given as

$$l_{\mathrm{Si}}(s) = 2r_i(\pi - \alpha_i(s)), i = 1, 2. \tag{S76}$$

In the equations above, $R(s)$ is the radius of the circle corresponding to the liquid surface arcs, and $\alpha_1(s)$, $\alpha_2(s)$ are the angles between the normal direction and the liquid-rod contact point. They are governed by these two implicit functions:

$$g = R\sum_{i=1,2}\cos(\theta_i + \alpha_i) + \sum_{i=1,2} r_i\cos\alpha_i, \tag{S77a}$$

$$\begin{aligned} A_L = &-\pi R^2 + \sum_{i=1,2}\left[\frac{1}{2}r_i^2\sin 2\alpha_i + 2r_i R\sin\alpha_i\cos(\theta_i + \alpha_i)\right], \\ &+ \sum_{i=1,2}\left[R^2(\theta_i + \alpha_i + \frac{1}{2}\sin(2\theta_i + 2\alpha_i)) - \alpha_i r_i^2\right]. \end{aligned} \tag{S77b}$$

S9 DERIVATION OF THE ANALYTIC FORM OF PLASTIC FLOW

The formulation of the temporal derivative of the left Cauchy-Green strain is given in (S12), which we use to evolve the left Cauchy-Green strain. This temporal derivative contains both the change through an elastic deformation and a plastic flow. Before solving the plastic flow, we have integrated the elastic deformation through $\bar{\mathbf{b}}^{E,*} = \bar{\mathbf{f}}\bar{\mathbf{b}}^E\bar{\mathbf{f}}^T$, where a bar is used to denote *volume-preserving* variables, e.g., $\bar{\mathbf{b}}^E$ is the *volume-preserving* left Cauchy-Green strain, and $\bar{\mathbf{f}}$ is the *volume-preserving* increment of the deformation gradient. Here, we only need to consider the change through a plastic flow in $\mathrm{d}\bar{\mathbf{b}}^E/\mathrm{d}t$, which is denoted $\mathrm{d}\bar{\mathbf{b}}^{E,*}/\mathrm{d}t$ and is formulated as

$$\frac{\mathrm{d}\bar{\mathbf{b}}^{E,*}}{\mathrm{d}t} = -\frac{2}{3}\mathrm{tr}(\bar{\mathbf{b}}^{E,*})\gamma(s^*)\hat{\mathbf{s}}^*. \tag{S78}$$

where $s^* \equiv \|\mathbf{s}^*\|$ and $\mathbf{s}^* \equiv \mu\mathrm{dev}\bar{\mathbf{b}}^{E,*}$ is the shear stress after the elastic deformation has been integrated. We further define the normalized shear stress $\hat{\mathbf{s}}^* \equiv \mathbf{s}^*/s^*$.

With some algebraic manipulations, we can rewrite $\bar{\mathbf{b}}^{E,*}$ from the definition of $\hat{\mathbf{s}}^*$, as

$$\bar{\mathbf{b}}^{E,*} = \frac{s^*}{\mu}\hat{\mathbf{s}}^* + \frac{1}{3}\mathrm{tr}(\bar{\mathbf{b}}^{E,*})\mathbf{I}_3 \tag{S79}$$

Taking the temperal derivative of both sides, we have

$$\frac{\mathrm{d}\bar{\mathbf{b}}^{E,*}}{\mathrm{d}t} = \mu^{-1}\left(\frac{\mathrm{d}s^*}{\mathrm{d}t}\hat{\mathbf{s}}^* + s^*\frac{\mathrm{d}\hat{\mathbf{s}}^*}{\mathrm{d}t}\right) + \frac{1}{3}\mathrm{tr}\left(\frac{\mathrm{d}\bar{\mathbf{b}}^{E,*}}{\mathrm{d}t}\right)\mathbf{I}_3 \tag{S80}$$

Since $\hat{\mathbf{s}}^*$ is deviatoric, $\mathrm{tr}(\hat{\mathbf{s}}^*) = 0$, we then have

$$\mathrm{tr}\left(\frac{\mathrm{d}\bar{\mathbf{b}}^{E,*}}{\mathrm{d}t}\right) = 0. \tag{S81}$$

Furthermore, during plastic flow the shear stress $\mathbf{s}^*$ can change in magnitude but *not in direction* due to the *principle of maximum plastic dissipation* [Simo 1988a], i.e.,

$$\frac{\mathrm{d}\hat{\mathbf{s}}^*}{\mathrm{d}t} = 0. \tag{S82}$$

Therefore, we have

$$\frac{\mathrm{d}\bar{\mathbf{b}}^{E,*}}{\mathrm{d}t} = \mu^{-1}\frac{\mathrm{d}s}{\mathrm{d}t}\hat{\mathbf{s}}^*. \tag{S83}$$

In other words, the temporal derivative of $\mathbf{b}^{E,*}$ can be computed directly from the temporal derivative of the magnitude of the shear stress s during plastic flow.

Comparing (S83) with (S78), we discover that

$$\frac{\mathrm{d}s^*}{\mathrm{d}t} = -2\hat{\mu}\gamma(s^*), \tag{S84}$$

where $\hat{\mu} \equiv \frac{\mu}{3}\mathrm{tr}\bar{\mathbf{b}}^{E,*}$. Assuming $\Phi(s)$ in (S13) will not change its sign during one time step, we then integrate s^* from time step t to $t+1$ through (S84) analytically, which gives us the form of (37).

S10 GRADIENT AND HESSIANS OF THE DISCRETE CURVATURES IN DISCRETE ELASTIC RODS

In this section, we derive the gradient and Hessians of the discrete curvature used in discrete elastic rod (DER). Although very lengthy, the Hessian is necessary when one implicitly integrates the bending force of DERs.

Motivation. In the literature, there are multiple models for DERs. The discrete curvatures (§S10.3) is initially defined in the *original work* of Bergou et al. [2008]. In a following work, Bergou et al. [2010] replaced these definition by projecting the curvature vector $\kappa\boldsymbol{b}$ to the neighbor material vectors $\boldsymbol{m}^{i-1}$ and $\boldsymbol{m}^i$ and combining the results. Although this latter form is simpler than their previous form proposed in 2008, i.e., the four terms used in their prior formulation of curvature [Bergou et al. 2008] are reduced to two terms, it is problematic — mathematically, it is meaningless to combine the $\kappa\boldsymbol{b}$ projected into different frames. Hence, in this paper, we still follow the original definition of discrete curvatures [Bergou et al. 2008], but replaced its space-parallel transport with a time-parallel transport when computing the reference vector. This formulation of DER is the same as the one taken by Kaldor et al. [2010]. Jawed et al. [2018] has presented a detailed derivation of the gradient and Hessian using the formulation in Bergou's later work [2010]. To help the potential readers to understand our implementation, we present a detailed derivation of the gradient and the Hessians of the discrete curvatures based on the correct formulation used by Kaldor et al. [2010], which has not been published anywhere else yet.

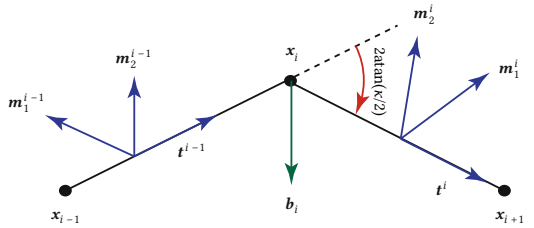

Fig. S2. **Discrete elastic rods**, adapted from the book by Jawed et al. [2018].

S10.1 Integrated Curvature Vector

We adopt the notations used in the book by Jawed et al. [2018]. The derivation begins with the definition of the integrated curvature vector $\kappa\boldsymbol{b}$ at a vertex i. Same as prior works [Bergou et al. 2008; Kaldor et al. 2010], we take the tangent of the half angle at vertex i as the discrete curvature.

$$(\kappa\boldsymbol{b})_i = \frac{2\boldsymbol{t}^{i-1}\times\boldsymbol{t}^i}{1+\boldsymbol{t}^{i-1}\cdot\boldsymbol{t}^i} = \frac{2\boldsymbol{e}^{i-1}\times\boldsymbol{e}^i}{\|\boldsymbol{e}^{i-1}\|\|\boldsymbol{e}^i\|+\boldsymbol{e}^{i-1}\cdot\boldsymbol{e}^i} \tag{S85}$$

where $\boldsymbol{t}^i$ is the normalized tangent vector at edge i, and $\boldsymbol{e}^i$ is the edge vector itself (so that $\boldsymbol{t}^i = \boldsymbol{e}^i/\|\boldsymbol{e}^i\|$).

We then derive the variation of this curvature vector, which has the following form

$$\begin{aligned}\delta(\kappa\boldsymbol{b})_i = &\frac{2\delta\boldsymbol{e}^{i-1}\times\boldsymbol{e}^i}{\|\boldsymbol{e}^{i-1}\|\|\boldsymbol{e}^i\|+\boldsymbol{e}^{i-1}\cdot\boldsymbol{e}^i} + \frac{2\boldsymbol{e}^{i-1}\times\delta\boldsymbol{e}^i}{\|\boldsymbol{e}^{i-1}\|\|\boldsymbol{e}^i\|+\boldsymbol{e}^{i-1}\cdot\boldsymbol{e}^i}\\ &- \frac{(\boldsymbol{e}^i+\|\boldsymbol{e}^i\|\boldsymbol{t}^{i-1})\cdot\delta\boldsymbol{e}^{i-1}}{\|\boldsymbol{e}^{i-1}\|\|\boldsymbol{e}^i\|+\boldsymbol{e}^{i-1}\cdot\boldsymbol{e}^i}(\kappa\boldsymbol{b})_i - \frac{(\boldsymbol{e}^{i-1}+\|\boldsymbol{e}^{i-1}\|\boldsymbol{t}^i)\cdot\delta\boldsymbol{e}^i}{\|\boldsymbol{e}^{i-1}\|\|\boldsymbol{e}^i\|+\boldsymbol{e}^{i-1}\cdot\boldsymbol{e}^i}(\kappa\boldsymbol{b})_i\end{aligned} \tag{S86}$$

By dividing by the magnitude of the edge vectors, we have

$$\begin{aligned}\delta(\kappa\boldsymbol{b})_i = &\frac{2\frac{\delta\boldsymbol{e}^{i-1}}{\|\boldsymbol{e}^{i-1}\|}\times\boldsymbol{t}^i}{1+\boldsymbol{t}^{i-1}\cdot\boldsymbol{t}^i} + \frac{2\boldsymbol{t}^{i-1}\times\frac{\delta\boldsymbol{e}^i}{\|\boldsymbol{e}^i\|}}{1+\boldsymbol{t}^{i-1}\cdot\boldsymbol{t}^i}\\ &- \frac{\boldsymbol{t}^{i-1}+\boldsymbol{t}^i}{1+\boldsymbol{t}^{i-1}\cdot\boldsymbol{t}^i}(\kappa\boldsymbol{b})_i\cdot\left(\frac{\delta\boldsymbol{e}^{i-1}}{\|\boldsymbol{e}^{i-1}\|}+\frac{\delta\boldsymbol{e}^i}{\|\boldsymbol{e}^i\|}\right)\end{aligned} \tag{S87}$$

S10.2 Material Vectors

We compute the variation of the material vectors $\boldsymbol{m}_1^i$ and $\boldsymbol{m}_2^i$ for defined at edge i. Following Jawed et al. [2018], the temporal derivative of the material vectors are

$$\dot{\boldsymbol{m}}_1^i(t) = \dot{\gamma}^i(t)\boldsymbol{m}_2^i(t) - \left(\boldsymbol{m}_1^i(t)\cdot\dot{\boldsymbol{t}}^i(t)\right)\boldsymbol{t}^i(t), \tag{S88a}$$

$$\dot{\boldsymbol{m}}_2^i(t) = -\dot{\gamma}^i(t)\boldsymbol{m}_1^i(t) - \left(\boldsymbol{m}_2^i(t)\cdot\dot{\boldsymbol{t}}^i(t)\right)\boldsymbol{t}^i(t). \tag{S88b}$$

where γ is the angle between *reference* vector and material vector, and only depends on the twist of rods. So the first term refects the change of twist along the complement material vector, and the second term reflects the change of direction of the edges. When

the position of vertices are disturbed, the change of twist $\dot{\gamma}$ is zero. Actually, we have

$$\delta \boldsymbol{m}_1^i = \delta\gamma^i \boldsymbol{m}_2^i - \left(\boldsymbol{m}_1^i \cdot \delta \boldsymbol{t}^i\right) \boldsymbol{t}^i, \tag{S89a}$$

$$\delta \boldsymbol{m}_2^i = -\delta\gamma^i \boldsymbol{m}_1^i - \left(\boldsymbol{m}_2^i \cdot \delta \boldsymbol{t}^i\right) \boldsymbol{t}^i. \tag{S89b}$$

S10.3 Discrete Curvatures

Our definition of discrete curvatures follows Kaldor et al. [2010], where one vertex at i generates four terms regards to its previous and next edges

$$\kappa_{i,1}^{i-1} = \boldsymbol{m}_2^{i-1} \cdot (\kappa \boldsymbol{b})_i, \tag{S90}$$

$$\kappa_{i,1}^{i} = \boldsymbol{m}_2^{i} \cdot (\kappa \boldsymbol{b})_i, \tag{S91}$$

$$\kappa_{i,2}^{i-1} = -\boldsymbol{m}_1^{i-1} \cdot (\kappa \boldsymbol{b})_i, \tag{S92}$$

$$\kappa_{i,2}^{i} = -\boldsymbol{m}_1^{i} \cdot (\kappa \boldsymbol{b})_i. \tag{S93}$$

We compute the variation of these curvatures, where we have

$$\delta\kappa_{i,1}^{i-1} = \boldsymbol{m}_2^{i-1} \cdot \delta(\kappa \boldsymbol{b})_i + \delta \boldsymbol{m}_2^{i-1} \cdot (\kappa \boldsymbol{b})_i, \tag{S94a}$$

$$\delta\kappa_{i,1}^{i} = \boldsymbol{m}_2^{i} \cdot \delta(\kappa \boldsymbol{b})_i + \delta \boldsymbol{m}_2^{i} \cdot (\kappa \boldsymbol{b})_i, \tag{S94b}$$

$$\delta\kappa_{i,2}^{i-1} = -\boldsymbol{m}_1^{i-1} \cdot \delta(\kappa \boldsymbol{b})_i - \delta \boldsymbol{m}_1^{i-1} \cdot (\kappa \boldsymbol{b})_i, \tag{S94c}$$

$$\delta\kappa_{i,2}^{i} = -\boldsymbol{m}_1^{i} \cdot \delta(\kappa \boldsymbol{b})_i - \delta \boldsymbol{m}_1^{i} \cdot (\kappa \boldsymbol{b})_i. \tag{S94d}$$

When only the positions of vertices are changing, we know from equation S89a that $\delta\gamma^i = 0$ and $\delta \boldsymbol{m}^i$ is parallel with the tangential direction $\boldsymbol{t}^i$. Hence $\delta \boldsymbol{m}^i$ is orthogonal with $(\kappa \boldsymbol{b})_i$. Therefore, we have the terms $\delta \boldsymbol{m}_1^i \cdot (\kappa \boldsymbol{b})_i = 0$ and $\delta \boldsymbol{m}_2^i \cdot (\kappa \boldsymbol{b})_i = 0$. For similar reason, $\delta \boldsymbol{m}_1^{i-1} \cdot (\kappa \boldsymbol{b})_i$ and $\delta \boldsymbol{m}_2^{i-1} \cdot (\kappa \boldsymbol{b})_i$ are also zero. We then have the following variations of curvatures

$$\delta\kappa_{i,1}^{i-1} = \boldsymbol{m}_2^{i-1} \cdot \delta(\kappa \boldsymbol{b})_i - \delta\gamma^{i-1} \boldsymbol{m}_1^{i-1} (\kappa \boldsymbol{b})_i, \tag{S95a}$$

$$\delta\kappa_{i,1}^{i} = \boldsymbol{m}_2^{i} \cdot \delta(\kappa \boldsymbol{b})_i - \delta\gamma^{i} \boldsymbol{m}_1^{i} (\kappa \boldsymbol{b})_i, \tag{S95b}$$

$$\delta\kappa_{i,2}^{i-1} = -\boldsymbol{m}_1^{i-1} \cdot \delta(\kappa \boldsymbol{b})_i - \delta\gamma^{i-1} \boldsymbol{m}_2^{i-1} (\kappa \boldsymbol{b})_i, \tag{S95c}$$

$$\delta\kappa_{i,2}^{i} = -\boldsymbol{m}_1^{i} \cdot \delta(\kappa \boldsymbol{b})_i - \delta\gamma^{i} \boldsymbol{m}_2^{i} (\kappa \boldsymbol{b})_i. \tag{S95d}$$

To compute the derivatives, we apply equation S87 to the variation of curvatures and set $\delta \boldsymbol{e}^{i-1}$, $\delta \boldsymbol{e}^{i}$, $\delta\gamma^{i-1}$ and $\delta\gamma^{i}$ to zero, respectively. We then have the following terms while the other terms are all zero

$$\frac{\partial \kappa_{i,1}^{i-1}}{\partial \boldsymbol{e}^{i-1}} \cdot \delta \boldsymbol{e}^{i-1} = \boldsymbol{m}_2^{i-1} \cdot \left[\frac{2 \frac{\delta \boldsymbol{e}^{i-1}}{\|\boldsymbol{e}^{i-1}\|} \times \boldsymbol{t}^i}{1 + \boldsymbol{t}^{i-1} \cdot \boldsymbol{t}^i} - \frac{\boldsymbol{t}^{i-1} + \boldsymbol{t}^i}{1 + \boldsymbol{t}^{i-1} \cdot \boldsymbol{t}^i} (\kappa \boldsymbol{b})_i \cdot \frac{\delta \boldsymbol{e}^{i-1}}{\|\boldsymbol{e}^{i-1}\|} \right], \tag{S96a}$$

$$\frac{\partial \kappa_{i,1}^{i-1}}{\partial \boldsymbol{e}^{i}} \cdot \delta \boldsymbol{e}^{i} = \boldsymbol{m}_2^{i-1} \cdot \left[\frac{2 \boldsymbol{t}^{i-1} \times \frac{\delta \boldsymbol{e}^{i}}{\|\boldsymbol{e}^{i}\|}}{1 + \boldsymbol{t}^{i-1} \cdot \boldsymbol{t}^i} - \frac{\boldsymbol{t}^{i-1} + \boldsymbol{t}^i}{1 + \boldsymbol{t}^{i-1} \cdot \boldsymbol{t}^i} (\kappa \boldsymbol{b})_i \cdot \frac{\delta \boldsymbol{e}^{i}}{\|\boldsymbol{e}^{i}\|} \right], \tag{S96b}$$

$$\frac{\partial \kappa_{i,1}^{i-1}}{\partial \gamma^{i-1}} \cdot \delta\gamma^{i-1} = -\delta\gamma^{i-1} \boldsymbol{m}_1^{i-1} (\kappa \boldsymbol{b})_i, \tag{S96c}$$

$$\frac{\partial \kappa_{i,1}^{i}}{\partial \boldsymbol{e}^{i-1}} \cdot \delta \boldsymbol{e}^{i-1} = \boldsymbol{m}_2^{i} \cdot \left[\frac{2 \frac{\delta \boldsymbol{e}^{i-1}}{\|\boldsymbol{e}^{i-1}\|} \times \boldsymbol{t}^i}{1 + \boldsymbol{t}^{i-1} \cdot \boldsymbol{t}^i} - \frac{\boldsymbol{t}^{i-1} + \boldsymbol{t}^i}{1 + \boldsymbol{t}^{i-1} \cdot \boldsymbol{t}^i} (\kappa \boldsymbol{b})_i \cdot \frac{\delta \boldsymbol{e}^{i-1}}{\|\boldsymbol{e}^{i-1}\|} \right], \tag{S96d}$$

$$\frac{\partial \kappa_{i,1}^{i}}{\partial \boldsymbol{e}^{i}} \cdot \delta \boldsymbol{e}^{i} = \boldsymbol{m}_2^{i} \cdot \left[\frac{2 \boldsymbol{t}^{i-1} \times \frac{\delta \boldsymbol{e}^{i}}{\|\boldsymbol{e}^{i}\|}}{1 + \boldsymbol{t}^{i-1} \cdot \boldsymbol{t}^i} - \frac{\boldsymbol{t}^{i-1} + \boldsymbol{t}^i}{1 + \boldsymbol{t}^{i-1} \cdot \boldsymbol{t}^i} (\kappa \boldsymbol{b})_i \cdot \frac{\delta \boldsymbol{e}^{i}}{\|\boldsymbol{e}^{i}\|} \right], \tag{S96e}$$

$$\frac{\partial \kappa_{i,1}^{i}}{\partial \gamma^{i}} \cdot \delta\gamma^{i} = -\delta\gamma^{i} \boldsymbol{m}_1^{i} (\kappa \boldsymbol{b})_i, \tag{S96f}$$

$$\frac{\partial \kappa_{i,2}^{i-1}}{\partial \boldsymbol{e}^{i-1}} \cdot \delta \boldsymbol{e}^{i-1} = -\boldsymbol{m}_1^{i-1} \cdot \left[\frac{2 \frac{\delta \boldsymbol{e}^{i-1}}{\|\boldsymbol{e}^{i-1}\|} \times \boldsymbol{t}^i}{1 + \boldsymbol{t}^{i-1} \cdot \boldsymbol{t}^i} - \frac{\boldsymbol{t}^{i-1} + \boldsymbol{t}^i}{1 + \boldsymbol{t}^{i-1} \cdot \boldsymbol{t}^i} (\kappa \boldsymbol{b})_i \cdot \frac{\delta \boldsymbol{e}^{i-1}}{\|\boldsymbol{e}^{i-1}\|} \right], \tag{S96g}$$

$$\frac{\partial \kappa_{i,2}^{i-1}}{\partial \boldsymbol{e}^{i}} \cdot \delta \boldsymbol{e}^{i} = -\boldsymbol{m}_1^{i-1} \cdot \left[\frac{2 \boldsymbol{t}^{i-1} \times \frac{\delta \boldsymbol{e}^{i}}{\|\boldsymbol{e}^{i}\|}}{1 + \boldsymbol{t}^{i-1} \cdot \boldsymbol{t}^i} - \frac{\boldsymbol{t}^{i-1} + \boldsymbol{t}^i}{1 + \boldsymbol{t}^{i-1} \cdot \boldsymbol{t}^i} (\kappa \boldsymbol{b})_i \cdot \frac{\delta \boldsymbol{e}^{i}}{\|\boldsymbol{e}^{i}\|} \right], \tag{S96h}$$

$$\frac{\partial \kappa_{i,2}^{i-1}}{\partial \gamma^{i-1}} \cdot \delta\gamma^{i-1} = -\delta\gamma^{i-1} \boldsymbol{m}_2^{i-1} (\kappa \boldsymbol{b})_i, \tag{S96i}$$

$$\frac{\partial \kappa_{i,2}^{i}}{\partial \boldsymbol{e}^{i-1}} \cdot \delta \boldsymbol{e}^{i-1} = -\boldsymbol{m}_1^{i} \cdot \left[\frac{2 \frac{\delta \boldsymbol{e}^{i-1}}{\|\boldsymbol{e}^{i-1}\|} \times \boldsymbol{t}^i}{1 + \boldsymbol{t}^{i-1} \cdot \boldsymbol{t}^i} - \frac{\boldsymbol{t}^{i-1} + \boldsymbol{t}^i}{1 + \boldsymbol{t}^{i-1} \cdot \boldsymbol{t}^i} (\kappa \boldsymbol{b})_i \cdot \frac{\delta \boldsymbol{e}^{i-1}}{\|\boldsymbol{e}^{i-1}\|} \right], \tag{S96j}$$

$$\frac{\partial \kappa_{i,2}^{i}}{\partial \boldsymbol{e}^{i}} \cdot \delta \boldsymbol{e}^{i} = -\boldsymbol{m}_1^{i} \cdot \left[\frac{2 \boldsymbol{t}^{i-1} \times \frac{\delta \boldsymbol{e}^{i}}{\|\boldsymbol{e}^{i}\|}}{1 + \boldsymbol{t}^{i-1} \cdot \boldsymbol{t}^i} - \frac{\boldsymbol{t}^{i-1} + \boldsymbol{t}^i}{1 + \boldsymbol{t}^{i-1} \cdot \boldsymbol{t}^i} (\kappa \boldsymbol{b})_i \cdot \frac{\delta \boldsymbol{e}^{i}}{\|\boldsymbol{e}^{i}\|} \right], \tag{S96k}$$

$$\frac{\partial \kappa_{i,2}^{i}}{\partial \gamma^{i}} \cdot \delta\gamma^{i} = -\delta\gamma^{i} \boldsymbol{m}_2^{i} (\kappa \boldsymbol{b})_i. \tag{S96l}$$

By using the rule of triple product and other algebraic manipulations, we achieve the following equations:

$$\frac{\partial \kappa_{i,1}^{i-1}}{\partial \boldsymbol{e}^{i-1}} = \frac{1}{\|\boldsymbol{e}^{i-1}\|} \left(-\kappa_{i,1}^{i-1} \tilde{\boldsymbol{t}} + \frac{2 \boldsymbol{t}^i \times \boldsymbol{m}_2^{i-1}}{1 + \boldsymbol{t}^{i-1} \cdot \boldsymbol{t}^i} \right), \tag{S97a}$$

$$\frac{\partial \kappa_{i,1}^{i-1}}{\partial \boldsymbol{e}^{i}} = \frac{1}{\|\boldsymbol{e}^{i}\|} \left(-\kappa_{i,1}^{i-1} \tilde{\boldsymbol{t}} - \frac{2 \boldsymbol{t}^{i-1} \times \boldsymbol{m}_2^{i-1}}{1 + \boldsymbol{t}^{i-1} \cdot \boldsymbol{t}^i} \right), \tag{S97b}$$

$$\frac{\partial \kappa_{i,1}^{i-1}}{\partial \gamma^{i-1}} = -\boldsymbol{m}_1^{i-1} (\kappa \boldsymbol{b})_i, \tag{S97c}$$

$$\frac{\partial \kappa_{i,1}^{i}}{\partial \boldsymbol{e}^{i-1}} = \frac{1}{\|\boldsymbol{e}^{i-1}\|} \left(-\kappa_{i,1}^{i} \tilde{\boldsymbol{t}} + \frac{2 \boldsymbol{t}^i \times \boldsymbol{m}_2^{i}}{1 + \boldsymbol{t}^{i-1} \cdot \boldsymbol{t}^i} \right), \tag{S97d}$$

$$\frac{\partial \kappa_{i,1}^{i}}{\partial \boldsymbol{e}^{i}} = \frac{1}{\|\boldsymbol{e}^{i}\|} \left(-\kappa_{i,1}^{i} \tilde{\boldsymbol{t}} - \frac{2 \boldsymbol{t}^{i-1} \times \boldsymbol{m}_2^{i}}{1 + \boldsymbol{t}^{i-1} \cdot \boldsymbol{t}^i} \right), \tag{S97e}$$

$$\frac{\partial \kappa_{i,1}^{i}}{\partial \gamma^{i}} = -\boldsymbol{m}_1^{i} (\kappa \boldsymbol{b})_i, \tag{S97f}$$

$$\frac{\partial \kappa_{i,2}^{i-1}}{\partial \boldsymbol{e}^{i-1}} = \frac{1}{\|\boldsymbol{e}^{i-1}\|}\left(-\kappa_{i,2}^{i-1}\tilde{\boldsymbol{t}} - \frac{2\boldsymbol{t}^i \times \boldsymbol{m}_1^{i-1}}{1+\boldsymbol{t}^{i-1}\cdot\boldsymbol{t}^i}\right), \tag{S97g}$$

$$\frac{\partial \kappa_{i,2}^{i-1}}{\partial \boldsymbol{e}^{i}} = \frac{1}{\|\boldsymbol{e}^{i}\|}\left(-\kappa_{i,2}^{i-1}\tilde{\boldsymbol{t}} + \frac{2\boldsymbol{t}^{i-1} \times \boldsymbol{m}_1^{i-1}}{1+\boldsymbol{t}^{i-1}\cdot\boldsymbol{t}^i}\right), \tag{S97h}$$

$$\frac{\partial \kappa_{i,2}^{i-1}}{\partial \gamma^{i-1}} = -\boldsymbol{m}_2^{i-1}(\kappa \boldsymbol{b})_i, \tag{S97i}$$

$$\frac{\partial \kappa_{i,2}^{i}}{\partial \boldsymbol{e}^{i-1}} = \frac{1}{\|\boldsymbol{e}^{i-1}\|}\left(-\kappa_{i,2}^{i}\tilde{\boldsymbol{t}} - \frac{2\boldsymbol{t}^i \times \boldsymbol{m}_1^{i}}{1+\boldsymbol{t}^{i-1}\cdot\boldsymbol{t}^i}\right), \tag{S97j}$$

$$\frac{\partial \kappa_{i,2}^{i}}{\partial \boldsymbol{e}^{i}} = \frac{1}{\|\boldsymbol{e}^{i}\|}\left(-\kappa_{i,2}^{i}\tilde{\boldsymbol{t}} + \frac{2\boldsymbol{t}^{i-1} \times \boldsymbol{m}_1^{i}}{1+\boldsymbol{t}^{i-1}\cdot\boldsymbol{t}^i}\right). \tag{S97k}$$

$$\frac{\partial \kappa_{i,2}^{i}}{\partial \gamma^{i}} = -\boldsymbol{m}_2^{i}(\kappa \boldsymbol{b})_i. \tag{S97l}$$

where $\tilde{\boldsymbol{t}} \equiv \frac{\boldsymbol{t}^{i-1}+\boldsymbol{t}^i}{1+\boldsymbol{t}^{i-1}\cdot\boldsymbol{t}^i}$.

S10.4 Hessian of the Discrete Curvatures

Before deriving the Hessian of the curvatures, it is convenient to define several variables and compute their derivatives, as following ($\otimes$ denotes the outer product, e.g., $\boldsymbol{a}\otimes\boldsymbol{b} \equiv \boldsymbol{a}\boldsymbol{b}^{\mathrm{T}}$.)

$$\frac{\partial \boldsymbol{t}^i}{\partial \boldsymbol{e}^i} = \frac{1}{\|\boldsymbol{e}^i\|}\left(\boldsymbol{I}_3 - \boldsymbol{t}^i\otimes\boldsymbol{t}^i\right) \tag{S98a}$$

$$\chi \equiv 1 + \boldsymbol{t}^{i-1}\cdot\boldsymbol{t}^i \tag{S98b}$$

$$\frac{\partial \chi}{\partial \boldsymbol{e}^{i-1}} = \frac{1}{\|\boldsymbol{e}^{i-1}\|}\left(\boldsymbol{I}_3 - \boldsymbol{t}^{k-1}\otimes\boldsymbol{t}^{k-1}\right)\boldsymbol{t}^k \tag{S98c}$$

$$\frac{\partial \chi}{\partial \boldsymbol{e}^{i}} = \frac{1}{\|\boldsymbol{e}^{i}\|}\left(\boldsymbol{I}_3 - \boldsymbol{t}^{k}\otimes\boldsymbol{t}^{k}\right)\boldsymbol{t}^{k-1} \tag{S98d}$$

$$\frac{\partial \tilde{\boldsymbol{t}}}{\partial \boldsymbol{e}^{i-1}} = \frac{1}{\chi\|\boldsymbol{e}^{i-1}\|}\left(\left(\boldsymbol{I}_3 - \boldsymbol{t}^{i-1}\otimes\boldsymbol{t}^{i-1}\right) - \tilde{t}\otimes\left(\left(\boldsymbol{I}_3 - \boldsymbol{t}^{i-1}\otimes\boldsymbol{t}^{i-1}\right)\boldsymbol{t}^i\right)\right) \tag{S98e}$$

$$\frac{\partial \tilde{\boldsymbol{t}}}{\partial \boldsymbol{e}^{i}} = \frac{1}{\chi\|\boldsymbol{e}^{i}\|}\left(\left(\boldsymbol{I}_3 - \boldsymbol{t}^{i}\otimes\boldsymbol{t}^{i}\right) - \tilde{t}\otimes\left(\left(\boldsymbol{I}_3 - \boldsymbol{t}^{i}\otimes\boldsymbol{t}^{i}\right)\boldsymbol{t}^{i-1}\right)\right) \tag{S98f}$$

Besides, we have

$$\frac{\partial}{\partial \boldsymbol{e}^i}(\boldsymbol{a}\times\boldsymbol{b}) = [\boldsymbol{a}]_\times\cdot\frac{\partial \boldsymbol{b}}{\partial \boldsymbol{e}^i} - [\boldsymbol{b}]_\times\cdot\frac{\partial \boldsymbol{a}}{\partial \boldsymbol{e}^i} \tag{S99}$$

for arbitrary vector $\boldsymbol{a}$ and $\boldsymbol{b}$, where the notation $[\cdot]_\times$ denotes the cross product matrix such that $\boldsymbol{a}\times\boldsymbol{b} = [\boldsymbol{a}]_\times\cdot\boldsymbol{b}$).

We then compute the Hessian of curvatures, where we have the following second derivative for the first line of (S97a),

$$\begin{aligned}\frac{\partial^2 \kappa_{i,1}^{i-1}}{\partial \boldsymbol{e}^{i-1}\partial \boldsymbol{e}^{i-1}} = &-\left(-\kappa_{i,1}^{i-1}\tilde{\boldsymbol{t}} + \frac{2\boldsymbol{t}^i\times\boldsymbol{m}_2^{i-1}}{\chi}\right)\otimes\frac{\boldsymbol{t}^{i-1}}{\|\boldsymbol{e}^{i-1}\|^2}\\ &+\frac{1}{\|\boldsymbol{e}^{i-1}\|}\left(-\frac{\partial \kappa_{i,1}^{i-1}}{\partial \boldsymbol{e}^{i-1}}\otimes\tilde{\boldsymbol{t}} - \kappa_{i,1}^{i-1}\frac{\partial \tilde{\boldsymbol{t}}}{\partial \boldsymbol{e}^{i-1}}\right.\\ &\left.-\frac{2[\boldsymbol{m}_2^{i-1}]_\times\cdot\frac{\partial \boldsymbol{t}^i}{\partial \boldsymbol{e}^{i-1}}}{\chi} - \frac{2\boldsymbol{t}^i\times\boldsymbol{m}_2^{i-1}}{\chi^2}\otimes\frac{\partial \chi}{\partial \boldsymbol{e}^{i-1}}\right),\end{aligned} \tag{S100}$$

Noticing that the first term of the above equation contains $\frac{\partial \kappa_{i,1}^{i-1}}{\partial \boldsymbol{e}^{i-1}}$, and $\frac{\partial \boldsymbol{t}^i}{\partial \boldsymbol{e}^{i-1}} = 0$, after combining the terms, we have

$$\begin{aligned}\frac{\partial^2 \kappa_{i,1}^{i-1}}{\partial \boldsymbol{e}^{i-1}\partial \boldsymbol{e}^{i-1}} = &-\frac{1}{\|\boldsymbol{e}^{i-1}\|}\left(\frac{\partial \kappa_{i,1}^{i-1}}{\partial \boldsymbol{e}^{i-1}}\otimes\boldsymbol{t}^{i-1} + \tilde{\boldsymbol{t}}\otimes\frac{\partial \kappa_{i,1}^{i-1}}{\partial \boldsymbol{e}^{i-1}}\right.\\ &\left.+\kappa_{i,1}^{i-1}\frac{\partial \tilde{\boldsymbol{t}}}{\partial \boldsymbol{e}^{i-1}} + \frac{2\boldsymbol{t}^i\times\boldsymbol{m}_2^{i-1}}{\chi^2}\otimes\frac{\partial \chi}{\partial \boldsymbol{e}^{i-1}}\right).\end{aligned} \tag{S101}$$

The Hessian matrix for this part is symmetric. We simplify it by combining the first and second terms. Also, we define

$$\tilde{\boldsymbol{m}}_2^{i-1} \equiv \frac{2\boldsymbol{m}_2^{i-1}}{\chi}, \tag{S102a}$$

$$\tilde{\boldsymbol{m}}_2^{i} \equiv \frac{2\boldsymbol{m}_2^{i}}{\chi}, \tag{S102b}$$

$$\tilde{\boldsymbol{m}}_1^{i-1} \equiv \frac{2\boldsymbol{m}_1^{i-1}}{\chi}, \tag{S102c}$$

$$\tilde{\boldsymbol{m}}_1^{i} \equiv \frac{2\boldsymbol{m}_1^{i}}{\chi}. \tag{S102d}$$

Before going on, remember that we also need the Hessians over the twisting angle γ. To compute these terms we note

$$\begin{aligned}\delta\left(\frac{\partial \kappa_{i,1}^{i-1}}{\partial \gamma^{i-1}}\right) &= -\delta\boldsymbol{m}_1^{i-1}(\kappa\boldsymbol{b})_i - \boldsymbol{m}_1^{i-1}\delta(\kappa\boldsymbol{b})_i\\ &= -\delta\gamma^{i-1}\boldsymbol{m}_2^{i-1}(\kappa\boldsymbol{b})_i - \boldsymbol{m}_1^{i-1}\delta(\kappa\boldsymbol{b})_i\end{aligned} \tag{S103}$$

We then derive other Hessians following a similar strategy for deriving (S101), and we use (S103) for the Hessians over γ. We have

$$\begin{aligned}\frac{\partial^2 \kappa_{i,1}^{i-1}}{\partial \boldsymbol{e}^{i-1}\partial \boldsymbol{e}^{i-1}} = &-\frac{1}{\|\boldsymbol{e}^{i-1}\|}\mathrm{sym}\left(\frac{\partial \kappa_{i,1}^{i-1}}{\partial \boldsymbol{e}^{i-1}}\otimes(\boldsymbol{t}^{i-1}+\tilde{\boldsymbol{t}})\right.\\ &\left.+\kappa_{i,1}^{i-1}\frac{\partial \tilde{\boldsymbol{t}}}{\partial \boldsymbol{e}^{i-1}} + \frac{1}{\chi}\left(\boldsymbol{t}^i\times\tilde{\boldsymbol{m}}_2^{i-1}\right)\otimes\frac{\partial \chi}{\partial \boldsymbol{e}^{i-1}}\right),\end{aligned} \tag{S104a}$$

$$\begin{aligned}\frac{\partial^2 \kappa_{i,1}^{i-1}}{\partial \boldsymbol{e}^{i}\partial \boldsymbol{e}^{i}} = &-\frac{1}{\|\boldsymbol{e}^{i}\|}\mathrm{sym}\left(\frac{\partial \kappa_{i,1}^{i-1}}{\partial \boldsymbol{e}^{i}}\otimes(\boldsymbol{t}^{i}+\tilde{\boldsymbol{t}})\right.\\ &\left.+\kappa_{i,1}^{i-1}\frac{\partial \tilde{\boldsymbol{t}}}{\partial \boldsymbol{e}^{i}} + \frac{1}{\chi}\left(\boldsymbol{t}^{i-1}\times\tilde{\boldsymbol{m}}_2^{i-1}\right)\otimes\frac{\partial \chi}{\partial \boldsymbol{e}^{i}}\right),\end{aligned} \tag{S104b}$$

$$\begin{aligned}\frac{\partial^2 \kappa_{i,1}^{i-1}}{\partial \boldsymbol{e}^{i}\partial \boldsymbol{e}^{i-1}} &= \left(\frac{\partial^2 \kappa_{i,1}^{i-1}}{\partial \boldsymbol{e}^{i-1}\partial \boldsymbol{e}^{i}}\right)^T\\ &= -\frac{1}{\|\boldsymbol{e}^{i-1}\|}\left(\tilde{\boldsymbol{t}}\otimes\frac{\partial \kappa_{i,1}^{i-1}}{\partial \boldsymbol{e}^{i}} + \kappa_{i,1}^{i-1}\frac{\partial \tilde{\boldsymbol{t}}}{\partial \boldsymbol{e}^{i}}\right.\\ &\left.+\frac{1}{\chi}\left(\boldsymbol{t}^i\times\tilde{\boldsymbol{m}}_2^{i-1}\right)\otimes\frac{\partial \chi}{\partial \boldsymbol{e}^{i}} + [\tilde{\boldsymbol{m}}_2^{i-1}]_\times\cdot\frac{\partial \boldsymbol{t}^i}{\partial \boldsymbol{e}^{i}}\right),\end{aligned} \tag{S104c}$$

$$\frac{\partial^2 \kappa_{i,1}^{i-1}}{\partial \boldsymbol{e}^{i-1}\partial \gamma^{i-1}} = \frac{1}{\|\boldsymbol{e}^{i-1}\|}\left(-\kappa_{i,2}^{i-1}\tilde{\boldsymbol{t}} - \boldsymbol{t}^i \times \tilde{\boldsymbol{m}}_1^{i-1}\right), \tag{S104d}$$

$$\frac{\partial^2 \kappa_{i,1}^{i-1}}{\partial \boldsymbol{e}^{i}\partial \gamma^{i-1}} = \frac{1}{\|\boldsymbol{e}^{i}\|}\left(-\kappa_{i,2}^{i-1}\tilde{\boldsymbol{t}} + \boldsymbol{t}^{i-1} \times \tilde{\boldsymbol{m}}_1^{i-1}\right), \tag{S104e}$$

$$\frac{\partial^2 \kappa_{i,1}^{i-1}}{\partial \gamma^{i-1}\partial \gamma^{i-1}} = -(\kappa \boldsymbol{b})_i \cdot \boldsymbol{m}_2^{i-1}, \tag{S104f}$$

$$\begin{aligned}\frac{\partial^2 \kappa_{i,2}^{i-1}}{\partial \boldsymbol{e}^{i-1}\partial \boldsymbol{e}^{i-1}} = &-\frac{1}{\|\boldsymbol{e}^{i-1}\|}\mathrm{sym}\left(\frac{\partial \kappa_{i,2}^{i-1}}{\partial \boldsymbol{e}^{i-1}} \otimes (\boldsymbol{t}^{i-1} + \tilde{\boldsymbol{t}})\right.\\ &\left.+\kappa_{i,2}^{i-1}\frac{\partial \tilde{\boldsymbol{t}}}{\partial \boldsymbol{e}^{i-1}} + \frac{1}{\chi}\left(\boldsymbol{t}^i \times \tilde{\boldsymbol{m}}_1^{i-1}\right) \otimes \frac{\partial \chi}{\partial \boldsymbol{e}^{i-1}}\right),\end{aligned} \tag{S104g}$$

$$\begin{aligned}\frac{\partial^2 \kappa_{i,2}^{i-1}}{\partial \boldsymbol{e}^{i}\partial \boldsymbol{e}^{i}} = &-\frac{1}{\|\boldsymbol{e}^{i}\|}\mathrm{sym}\left(\frac{\partial \kappa_{i,2}^{i-1}}{\partial \boldsymbol{e}^{i}} \otimes (\boldsymbol{t}^{i} + \tilde{\boldsymbol{t}})\right.\\ &\left.+\kappa_{i,2}^{i-1}\frac{\partial \tilde{\boldsymbol{t}}}{\partial \boldsymbol{e}^{i}} + \frac{1}{\chi}\left(\boldsymbol{t}^{i-1} \times \tilde{\boldsymbol{m}}_1^{i-1}\right) \otimes \frac{\partial \chi}{\partial \boldsymbol{e}^{i}}\right),\end{aligned} \tag{S104h}$$

$$\begin{aligned}\frac{\partial^2 \kappa_{i,2}^{i-1}}{\partial \boldsymbol{e}^{i}\partial \boldsymbol{e}^{i-1}} &= \left(\frac{\partial^2 \kappa_{i,2}^{i-1}}{\partial \boldsymbol{e}^{i-1}\partial \boldsymbol{e}^{i}}\right)^T\\ &= -\frac{1}{\|\boldsymbol{e}^{i-1}\|}\left(\tilde{\boldsymbol{t}} \otimes \frac{\partial \kappa_{i,2}^{i-1}}{\partial \boldsymbol{e}^{i}} + \kappa_{i,2}^{i-1}\frac{\partial \tilde{\boldsymbol{t}}}{\partial \boldsymbol{e}^{i}}\right.\\ &\left.-\frac{1}{\chi}\left(\boldsymbol{t}^i \times \tilde{\boldsymbol{m}}_1^{i-1}\right) \otimes \frac{\partial \chi}{\partial \boldsymbol{e}^{i}} - [\tilde{\boldsymbol{m}}_1^{i-1}]_\times \cdot \frac{\partial \boldsymbol{t}^i}{\partial \boldsymbol{e}^{i}}\right),\end{aligned} \tag{S104i}$$

$$\frac{\partial^2 \kappa_{i,2}^{i-1}}{\partial \boldsymbol{e}^{i-1}\partial \gamma^{i-1}} = \frac{1}{\|\boldsymbol{e}^{i-1}\|}\left(\kappa_{i,1}^{i-1}\tilde{\boldsymbol{t}} - \boldsymbol{t}^i \times \tilde{\boldsymbol{m}}_2^{i-1}\right), \tag{S104j}$$

$$\frac{\partial^2 \kappa_{i,2}^{i-1}}{\partial \boldsymbol{e}^{i}\partial \gamma^{i-1}} = \frac{1}{\|\boldsymbol{e}^{i}\|}\left(\kappa_{i,1}^{i-1}\tilde{\boldsymbol{t}} + \boldsymbol{t}^{i-1} \times \tilde{\boldsymbol{m}}_2^{i-1}\right), \tag{S104k}$$

$$\frac{\partial^2 \kappa_{i,2}^{i-1}}{\partial \gamma^{i-1}\partial \gamma^{i-1}} = (\kappa \boldsymbol{b})_i \cdot \boldsymbol{m}_1^{i-1}, \tag{S104l}$$

$$\begin{aligned}\frac{\partial^2 \kappa_{i,1}^{i}}{\partial \boldsymbol{e}^{i-1}\partial \boldsymbol{e}^{i-1}} = &-\frac{1}{\|\boldsymbol{e}^{i-1}\|}\mathrm{sym}\left(\frac{\partial \kappa_{i,1}^{i}}{\partial \boldsymbol{e}^{i-1}} \otimes (\boldsymbol{t}^{i-1} + \tilde{\boldsymbol{t}})\right.\\ &\left.+\kappa_{i,1}^{i}\frac{\partial \tilde{\boldsymbol{t}}}{\partial \boldsymbol{e}^{i-1}} + \frac{1}{\chi}\left(\boldsymbol{t}^i \times \tilde{\boldsymbol{m}}_2^{i}\right) \otimes \frac{\partial \chi}{\partial \boldsymbol{e}^{i-1}}\right),\end{aligned} \tag{S104m}$$

$$\begin{aligned}\frac{\partial^2 \kappa_{i,1}^{i}}{\partial \boldsymbol{e}^{i}\partial \boldsymbol{e}^{i}} = &-\frac{1}{\|\boldsymbol{e}^{i}\|}\mathrm{sym}\left(\frac{\partial \kappa_{i,1}^{i}}{\partial \boldsymbol{e}^{i}} \otimes (\boldsymbol{t}^{i} + \tilde{\boldsymbol{t}})\right.\\ &\left.+\kappa_{i,1}^{i}\frac{\partial \tilde{\boldsymbol{t}}}{\partial \boldsymbol{e}^{i}} + \frac{1}{\chi}\left(\boldsymbol{t}^{i-1} \times \tilde{\boldsymbol{m}}_2^{i}\right) \otimes \frac{\partial \chi}{\partial \boldsymbol{e}^{i}}\right),\end{aligned} \tag{S104n}$$

$$\begin{aligned}\frac{\partial^2 \kappa_{i,1}^{i}}{\partial \boldsymbol{e}^{i}\partial \boldsymbol{e}^{i-1}} &= \left(\frac{\partial^2 \kappa_{i,1}^{i}}{\partial \boldsymbol{e}^{i-1}\partial \boldsymbol{e}^{i}}\right)^T\\ &= -\frac{1}{\|\boldsymbol{e}^{i-1}\|}\left(\tilde{\boldsymbol{t}} \otimes \frac{\partial \kappa_{i,1}^{i}}{\partial \boldsymbol{e}^{i}} + \kappa_{i,1}^{i}\frac{\partial \tilde{\boldsymbol{t}}}{\partial \boldsymbol{e}^{i}}\right.\\ &\left.+\frac{1}{\chi}\left(\boldsymbol{t}^i \times \tilde{\boldsymbol{m}}_2^{i}\right) \otimes \frac{\partial \chi}{\partial \boldsymbol{e}^{i}} + [\tilde{\boldsymbol{m}}_2^{i}]_\times \cdot \frac{\partial \boldsymbol{t}^i}{\partial \boldsymbol{e}^{i}}\right),\end{aligned} \tag{S104o}$$

$$\frac{\partial^2 \kappa_{i,1}^{i}}{\partial \boldsymbol{e}^{i-1}\partial \gamma^{i}} = \frac{1}{\|\boldsymbol{e}^{i-1}\|}\left(-\kappa_{i,2}^{i}\tilde{\boldsymbol{t}} - \boldsymbol{t}^i \times \tilde{\boldsymbol{m}}_1^{i}\right), \tag{S104p}$$

$$\frac{\partial^2 \kappa_{i,1}^{i}}{\partial \boldsymbol{e}^{i}\partial \gamma^{i}} = \frac{1}{\|\boldsymbol{e}^{i}\|}\left(-\kappa_{i,2}^{i}\tilde{\boldsymbol{t}} + \boldsymbol{t}^{i-1} \times \tilde{\boldsymbol{m}}_1^{i}\right), \tag{S104q}$$

$$\frac{\partial^2 \kappa_{i,1}^{i}}{\partial \gamma^{i}\partial \gamma^{i}} = -(\kappa \boldsymbol{b})_i \cdot \boldsymbol{m}_2^{i}, \tag{S104r}$$

$$\begin{aligned}\frac{\partial^2 \kappa_{i,2}^{i}}{\partial \boldsymbol{e}^{i-1}\partial \boldsymbol{e}^{i-1}} = &-\frac{1}{\|\boldsymbol{e}^{i-1}\|}\mathrm{sym}\left(\frac{\partial \kappa_{i,2}^{i}}{\partial \boldsymbol{e}^{i-1}} \otimes (\boldsymbol{t}^{i-1} + \tilde{\boldsymbol{t}})\right.\\ &\left.+\kappa_{i,2}^{i}\frac{\partial \tilde{\boldsymbol{t}}}{\partial \boldsymbol{e}^{i-1}} + \frac{1}{\chi}\left(\boldsymbol{t}^i \times \tilde{\boldsymbol{m}}_1^{i}\right) \otimes \frac{\partial \chi}{\partial \boldsymbol{e}^{i-1}}\right),\end{aligned} \tag{S104s}$$

$$\begin{aligned}\frac{\partial^2 \kappa_{i,2}^{i}}{\partial \boldsymbol{e}^{i}\partial \boldsymbol{e}^{i}} = &-\frac{1}{\|\boldsymbol{e}^{i}\|}\mathrm{sym}\left(\frac{\partial \kappa_{i,2}^{i}}{\partial \boldsymbol{e}^{i}} \otimes (\boldsymbol{t}^{i} + \tilde{\boldsymbol{t}})\right.\\ &\left.+\kappa_{i,2}^{i}\frac{\partial \tilde{\boldsymbol{t}}}{\partial \boldsymbol{e}^{i}} + \frac{1}{\chi}\left(\boldsymbol{t}^{i-1} \times \tilde{\boldsymbol{m}}_1^{i}\right) \otimes \frac{\partial \chi}{\partial \boldsymbol{e}^{i}}\right),\end{aligned} \tag{S104t}$$

$$\begin{aligned}\frac{\partial^2 \kappa_{i,2}^{i}}{\partial \boldsymbol{e}^{i}\partial \boldsymbol{e}^{i-1}} &= \left(\frac{\partial^2 \kappa_{i,2}^{i}}{\partial \boldsymbol{e}^{i-1}\partial \boldsymbol{e}^{i}}\right)^T\\ &= -\frac{1}{\|\boldsymbol{e}^{i-1}\|}\left(\tilde{\boldsymbol{t}} \otimes \frac{\partial \kappa_{i,2}^{i}}{\partial \boldsymbol{e}^{i}} + \kappa_{i,2}^{i}\frac{\partial \tilde{\boldsymbol{t}}}{\partial \boldsymbol{e}^{i}}\right.\\ &\left.-\frac{1}{\chi}\left(\boldsymbol{t}^i \times \tilde{\boldsymbol{m}}_1^{i}\right) \otimes \frac{\partial \chi}{\partial \boldsymbol{e}^{i}} - [\tilde{\boldsymbol{m}}_1^{i}]_\times \cdot \frac{\partial \boldsymbol{t}^i}{\partial \boldsymbol{e}^{i}}\right).\end{aligned} \tag{S104u}$$

$$\frac{\partial^2 \kappa_{i,2}^{i}}{\partial \boldsymbol{e}^{i-1}\partial \gamma^{i}} = \frac{1}{\|\boldsymbol{e}^{i-1}\|}\left(\kappa_{i,1}^{i}\tilde{\boldsymbol{t}} - \boldsymbol{t}^i \times \tilde{\boldsymbol{m}}_2^{i}\right), \tag{S104v}$$

$$\frac{\partial^2 \kappa_{i,2}^{i}}{\partial \boldsymbol{e}^{i}\partial \gamma^{i}} = \frac{1}{\|\boldsymbol{e}^{i}\|}\left(\kappa_{i,1}^{i}\tilde{\boldsymbol{t}} + \boldsymbol{t}^{i-1} \times \tilde{\boldsymbol{m}}_2^{i}\right), \tag{S104w}$$

$$\frac{\partial^2 \kappa_{i,2}^{i}}{\partial \gamma^{i}\partial \gamma^{i}} = (\kappa \boldsymbol{b})_i \cdot \boldsymbol{m}_1^{i}, \tag{S104x}$$

where we use the notation $\mathrm{sym}(\boldsymbol{A}) \equiv (\boldsymbol{A}+\boldsymbol{A}^T)/2$. The Hessian terms other than the ones above are all zero filled.

The total bending energy for a strand is then defined over curvatures

$$E_b = \frac{1}{4}\sum_i \sum_{j=0,1} [\kappa_{i,1}^{i-j} - \bar{\kappa}_{i,1}^{i-j}, \kappa_{i,2}^{i-j} - \bar{\kappa}_{i,2}^{i-j}] B_i [\kappa_{i,1}^{i-j} - \bar{\kappa}_{i,1}^{i-j}, \kappa_{i,2}^{i-j} - \bar{\kappa}_{i,2}^{i-j}]^T. \tag{S105}$$

where $B_i \in \mathbb{R}^{2\times 2}$ is the bending stiffness tensor at vertex i, and the variables with a bar denote the rest states. With the gradient and Hessians of curvatures given above, the bending force and its Jacobian can be trivially computed, following Kaldor et al. [2010].

S11 JACOBIAN OF LIQUID'S SHEAR FORCE

In the augmented MLS-MPM method, the i-th row and j-th column of the Jacobian matrix of the shear force $\mathbf{H}_\mathrm{f}$ is computed as [Hu et al. 2018; Stomakhin et al. 2014]

$$\mathbf{H}_{\mathrm{f,ij}} = \sum_p V_p^0 \boldsymbol{e}_i^\mathrm{T} \boldsymbol{L}_{p,j} (\mathbf{F}_p^E)^\mathrm{T} \mathbf{D}_p^{-1} N_i(\boldsymbol{x}_p)(\boldsymbol{x}_{f,i} - \boldsymbol{x}_p) \tag{S106}$$

where

$$\boldsymbol{L}_{p,j} \equiv \frac{\partial^2 W_{\mathrm{s}}}{\partial \mathbf{F} \partial \mathbf{F}} : \mathbf{D}_p^{-1} N_j(\boldsymbol{x}_p) \boldsymbol{e}_j (\boldsymbol{x}_{f,j} - \boldsymbol{x}_p)^{\mathrm{T}} \mathbf{F}_p^E. \tag{S107}$$

In the equations above, $N_i(\boldsymbol{x}_p)$ is the B-spline kernel evaluated at the position $\boldsymbol{x}_p$ of particle p; $\boldsymbol{x}_{f,i}$ is the central position of grid face i; $\boldsymbol{e}_i$ is the normal direction of grid face i; $\mathbf{D}_p$ is the inertia tensor of the kernel function; $\mathrm{dev}(\mathbf{b}_p^{E,t})$ is the deviatoric part of the left Cauchy-Green strain tensor $\mathbf{b}_p^{E,t}$ (see §S1); and the operator $\boldsymbol{A} : \mathbf{B}$ denotes the tensor product between a fourth-order tensor $\boldsymbol{A}$ and a second-order tensor $\mathbf{B}$. We then need to insert our Herschel-Bulkley model into these equations. Below we derive a general Jacobian matrix for 2D and 3D, with the number of dimensions denoted as d, i.e., $d = 2$ for 2D and $d = 3$ for 3D.

We begin our derivation from (S6), where we have the derivative of shear energy over $\mathbf{F}^E$:

$$\frac{\partial W_{\mathrm{s}}}{\partial \mathbf{F}_{ij}^E} = \mu \mathrm{dev}(\bar{\mathbf{b}}^E) \mathbf{F}^{E-\mathrm{T}}. \tag{S108}$$

where a bar indicates normalized variables, and $\bar{\mathbf{b}}^E = J^{-2/d} \mathbf{F}^E \mathbf{F}^{E\mathrm{T}}$ is the normalized left Cauchy-Green strain tensor. We define a function λ to represent the plastic flow, i.e., rewriting (37) as $s^{t+1} = \lambda(s^*, \hat{\mu})$.

Below we drop the star and E superscripts for brevity. We have $\bar{\mathbf{b}} = \frac{\lambda(s,\hat{\mu})}{s} \mathrm{dev}(\bar{\mathbf{b}}) + \hat{\mu} \mathbf{I}_3$ and thence $\mathrm{dev}(\bar{\mathbf{b}}) = \frac{\lambda(s,\hat{\mu})}{s} \mathrm{dev}(\bar{\mathbf{b}})$, and

$$\frac{\partial W_{\mathrm{s}}}{\partial \mathbf{F}_{ij}} = \mu \tilde{\lambda} J^{-2/d} \left[\mathbf{F}_{ij} - \frac{1}{d} \mathrm{tr}\left(\mathbf{F}\mathbf{F}^{\mathrm{T}}\right) \left(\mathbf{F}^{-\mathrm{T}}\right)_{ij} \right]. \tag{S109}$$

where $\tilde{\lambda} \equiv \frac{\lambda(s,\hat{\mu})}{s}$. Applying matrix calculus [Petersen et al. 2008], we have the following derivatives:

$$\frac{\partial J^{-2/d}}{\partial \mathbf{F}_{uv}} = -\frac{2}{d} J^{-2/d} (\mathbf{F}^{-\mathrm{T}})_{uv}, \tag{S110a}$$

$$\frac{\partial \mathbf{F}_{ij}}{\partial \mathbf{F}_{uv}} = \delta_{ui} \delta_{jv}, \tag{S110b}$$

$$\frac{\partial}{\partial \mathbf{F}_{uv}} \mathrm{tr}\left(\mathbf{F}\mathbf{F}^{\mathrm{T}}\right) = \mathbf{F}_{uv}, \tag{S110c}$$

$$\frac{\partial}{\partial \mathbf{F}_{uv}} \left(\mathbf{F}^{-\mathrm{T}}\right)_{ij} = \frac{\partial}{\partial \mathbf{F}_{uv}} \left(\mathbf{F}^{-1}\right)_{ji} = -\left(\mathbf{F}^{-1}\right)_{ju} \left(\mathbf{F}^{-1}\right)_{vi}. \tag{S110d}$$

where δ_{ij} is the Kronecker delta, i.e., $\delta_{ij} = 1$ if and only if $i = j$.

By the chain rule, we can compute

$$\frac{\partial s}{\partial \mathbf{s}} = \frac{\mathbf{s}}{s}, \tag{S111a}$$

$$\frac{\partial \mathbf{s}_{ij}}{\partial \mathbf{F}_{uv}} = \mu J^{-2/d} \left[-\frac{2}{d} (\mathbf{F}^{-T})_{uv} [\mathrm{dev}\mathbf{b}]_{ij} + \delta_{iu} \mathbf{F}_{jv} - \frac{1}{d} \mathbf{F}_{uv} \delta_{ij} \right], \tag{S111b}$$

$$\frac{\partial s}{\partial \mathbf{F}_{uv}} = -\frac{2s}{d} (\mathbf{F}^{-T})_{uv} + \mu \frac{(\mathrm{dev}\bar{\mathbf{b}} \cdot \mathbf{F})_{uv} - \frac{1}{d} \mathrm{tr}(\mathrm{dev}\bar{\mathbf{b}})}{\|\mathrm{dev}\bar{\mathbf{b}}\|}, \tag{S111c}$$

$$\frac{\partial \hat{\mu}}{\partial \mathbf{F}_{uv}} = \frac{1}{d} \mu J^{-2/d} \left[-\frac{2}{d} (\mathbf{F}^{-T})_{uv} \mathrm{tr}\mathbf{b} + \mathbf{F}_{uv} \right]. \tag{S111d}$$

The Hessian of the shear energy then becomes

$$\begin{aligned}
&\frac{\partial}{\partial \mathbf{F}_{uv}} \left(\frac{\partial W_{\mathrm{s}}}{\partial \mathbf{F}_{ij}} \right) \\
&= -\frac{2}{d} J^{-2/d} (\mathbf{F}^{-\mathrm{T}})_{uv} \left[\mathbf{F}_{ij} - \frac{1}{d} \mathrm{tr}\left(\mathbf{F}\mathbf{F}^{\mathrm{T}}\right) \left(\mathbf{F}^{-\mathrm{T}}\right)_{ij} \right] \\
&+ \mu J^{-2/d} \left[\delta_{ui}\delta_{jv} - \frac{1}{d} \left(\mathbf{F}_{uv} \mathbf{F}_{ij}^{-\mathrm{T}} - \mathrm{tr}\left(\mathbf{F}\mathbf{F}^{\mathrm{T}}\right) \left(\mathbf{F}^{-1}\right)_{ju} \left(\mathbf{F}^{-1}\right)_{vi} \right) \right] \\
&+ \left[\mu J^{-2/d} \left[\mathbf{F}_{ij} - \frac{1}{d} \mathrm{tr}\left(\mathbf{F}\mathbf{F}^{\mathrm{T}}\right) \left(\mathbf{F}^{-\mathrm{T}}\right)_{ij} \right] \right] \\
&\left[\frac{\partial \tilde{\lambda}}{\partial s} \left(-\frac{2s}{d} (\mathbf{F}^{-T})_{uv} + \mu \frac{(\mathrm{dev}\bar{\mathbf{b}} \cdot \mathbf{F})_{uv}}{\|\mathrm{dev}\bar{\mathbf{b}}\|} \right) \right. \\
&\left. + \frac{\partial \tilde{\lambda}}{\partial \mu} \frac{\mu}{d} J^{-2/d} \left(-\frac{2}{d} (\mathbf{F}^{-T})_{uv} \mathrm{tr}\mathbf{b} + \mathbf{F}_{uv} \right) \right].
\end{aligned} \tag{S112}$$

In addition, for an arbitrary matrix $\mathbf{B} \in \mathbb{R}^{d \times d}$, under the Einstein notation we have [Petersen et al. 2008]

$$\delta_{ui}\delta_{jv} \mathbf{B}_{uv} = \mathbf{B}_{ij}, \tag{S113a}$$

$$\mathbf{F}_{uv} \mathbf{B}_{uv} = \mathrm{tr}(\mathbf{F}^{\mathrm{T}} \mathbf{B}), \tag{S113b}$$

$$\left(\mathbf{F}^{-1}\right)_{ju} \left(\mathbf{F}^{-1}\right)_{vi} \mathbf{B}_{uv} = \left(\mathbf{F}^{-\mathrm{T}} \mathbf{B}^{\mathrm{T}} \mathbf{F}^{-\mathrm{T}}\right)_{ij}, \tag{S113c}$$

$$\left(\frac{\partial^2 W_{\mathrm{s}}}{\partial \mathbf{F} \partial \mathbf{F}} : \mathbf{B} \right)_{ij} \equiv \frac{\partial}{\partial \mathbf{F}_{uv}} \left(\frac{\partial W_{\mathrm{s}}}{\partial \mathbf{F}_{ij}} \right) \mathbf{B}_{uv}. \tag{S113d}$$

Using these equations and some algebra operations, we have the following formulation for multiplying the Hessian of shear energy with an arbitrary matrix $\mathbf{B}$:

$$\begin{aligned}
\frac{\partial^2 W_{\mathrm{s}}}{\partial \mathbf{F} \partial \mathbf{F}} : \mathbf{B} = \mu &\left[J^{-2/d} \mathbf{B} - \frac{2}{d} \mathrm{tr}\left(\mathbf{F}^{-1}\mathbf{B}\right) \mathrm{dev}\left(\bar{\mathbf{b}}\right) \mathbf{F}^{-\mathrm{T}} \right. \\
&\left. - \frac{1}{d} \mathbf{F}^{-\mathrm{T}} \left(J^{-2/d} \mathrm{tr}\left(\mathbf{F}^{\mathrm{T}}\mathbf{B}\right) \mathbf{I}_d - \mathrm{tr}\left(\bar{\mathbf{b}}\right) \mathbf{B}^{\mathrm{T}} \mathbf{F}^{-\mathrm{T}} \right) \right] \\
&+ \mu \mathrm{dev}\bar{\mathbf{b}} \cdot \mathbf{F}^{-T} \left[\frac{\partial \tilde{\lambda}}{\partial s} \left(-\frac{2s}{d} \mathrm{tr}(\mathbf{F}^{-1}\mathbf{B}) + \mu \frac{\mathrm{tr}(\mathbf{F}^T \mathrm{dev}\bar{\mathbf{b}} \cdot \mathbf{B})}{\|\mathrm{dev}\bar{\mathbf{b}}\|} \right) \right. \\
&\left. + \frac{\partial \tilde{\lambda}}{\partial \mu} \frac{\mu}{d} J^{-2/d} \left(-\frac{2}{d} \mathrm{tr}(\mathbf{F}^{-1}\mathbf{B}) \mathrm{tr}\mathbf{b} + \mathrm{tr}(\mathbf{F}^T\mathbf{B}) \right) \right]
\end{aligned} \tag{S114}$$

Explicitly computing (S114) and constructing a Jacobian matrix is not economically efficient. Instead, only computing the result of multiplying the Jacobian with a vector is more effective, similar to prior works [Hu et al. 2018; Stomakhin et al. 2014] (e.g., in (34) that implicitly integrates the shear stress, the vector to be multiplied with is the velocity $\boldsymbol{u}_{\mathrm{f}}^*$ or some intermediate states in a conjugate gradient solver). Noticing that the deformation gradient $\mathbf{F}$ can be canceled or combined into $\bar{\mathbf{b}}$ when substituting (S114) into (S107) and (S106), then the multiplication between the Jacobian matrix $\mathbf{H}_{\mathrm{f}}$ and an arbitrary vector $\boldsymbol{q}$ (whose dimension matches the number of columns of $\mathbf{H}_{\mathrm{f}}$) can be computed below.

Defining

$$\boldsymbol{v}_{j\alpha,p} \equiv N_{j\alpha}(\boldsymbol{x}_p)(\boldsymbol{x}_{\mathrm{f},j\alpha} - \boldsymbol{x}_p) \tag{S115}$$

for direction $\alpha \in [0, d-1]$, in 2D we define

$$\mathbf{B}_p \equiv \sum_j [\boldsymbol{v}_{j0,p}\boldsymbol{q}_{j0}, \boldsymbol{v}_{j1,p}\boldsymbol{q}_{j1}]. \tag{S116}$$

and in 3D

$$\mathbf{B}_p \equiv \sum_j [\boldsymbol{v}_{j0,p}\boldsymbol{q}_{j0}, \boldsymbol{v}_{j1,p}\boldsymbol{q}_{j1}, \boldsymbol{v}_{j2,p}\boldsymbol{q}_{j2}]. \tag{S117}$$

With all the variables defined above substituted into (S106), and using $\mathbf{B}_p$ to replace the arbitrary matrix $\mathbf{B}$ in (S114), the Jacobian matrix multiplied with an arbitrary vector $\boldsymbol{q}$ is computed as

$$(\mathbf{H}_\mathrm{f}\boldsymbol{q})_{i\alpha} = \sum_p \tilde{\boldsymbol{L}}_{p,\alpha *}\boldsymbol{v}_{i\alpha,p} \tag{S118}$$

where $\tilde{\boldsymbol{L}}_{p,\alpha *} \in \mathbb{R}^{1\times d}$ is the α-row of $\tilde{\boldsymbol{L}}_p$, and

$$\begin{aligned}\tilde{\boldsymbol{L}}_p \equiv \mu V_p^0 \mathbf{D}_p^{-2} \Bigg[& s^{t+1}\left(\mathbf{B}_p^{\mathrm{T}}\bar{\mathbf{b}} - \frac{2}{d}\mathrm{tr}(\mathbf{B}_p)\mathrm{dev}(\bar{\mathbf{b}})\right. \\ & \left. -\frac{1}{d}\left(\left(\mathbf{B}_p \odot \bar{\mathbf{b}}\right)\mathbf{I}_d - \mathrm{tr}(\bar{\mathbf{b}})\mathbf{B}_p\right)\right) \\ & +\mathrm{dev}(\bar{\mathbf{b}})\left(\frac{\partial\tilde{\lambda}}{\partial s}\left(\frac{\mu\mathrm{tr}(\mathrm{dev}(\bar{\mathbf{b}})\mathbf{B}_p^T\bar{\mathbf{b}})}{\|\mathrm{dev}\bar{\mathbf{b}}\|} - \frac{2s^{t+1}}{d}\right)\right. \\ & \left.+\frac{\partial\tilde{\lambda}}{\partial\mu}\frac{\mu}{d}\left(\mathrm{tr}(\mathbf{B}_p^T\bar{\mathbf{b}}) - \frac{2}{d}\mathrm{tr}(\mathbf{B}_p)\mathrm{tr}(\bar{\mathbf{b}})\right)\right)\Bigg],\end{aligned} \tag{S119}$$

where $\odot$ denotes the Frobenius inner product, i.e., $\boldsymbol{A}\odot\mathbf{B} = \sum_i\sum_j A_{ij}B_{ij}$.

S12 A SINGLE STEP OF OUR ALGORITHM

A single step of our complete algorithm consists of the following sequence of operations:

(1) **Transfer between surface and bulk liquid.** Bulk liquid is captured as surface flow for those strands crossing the interface; excess liquid from surface flow is converted into particles.
(2) **Merge, split, and relax particles.** Following Winchenbach et al. [2017], particles that are too small are merged with neighbor particles, while ones that are too large are split. In addition, we apply a pass of relaxation [Ando et al. 2012] to maintain the uniformity of the particle distribution.
(3) **Map liquid particles to grid.** At the start of every time step we transfer the particles' mass, velocity, and volume change to the MAC grid, through the APIC method [Jiang et al. 2015].
(4) **Compute weighting and gradient matrices.** The weighting and gradient matrices in Table 1 are computed, for both liquid and strands.
(5) **Detect tearing regions.** Each particle's accumulated plasticity is examined to detect tearing [Yue et al. 2015].
(6) **Solve for Mixture.** The velocities of the grid, surface flow, and strands are updated, following Algorithm 1. The shear equation (34) is solved with a Jacobi preconditioned conjugate gradient solver [Saad 2003], and the pressure equation (38) is solved with an algebraic multigrid preconditioned conjugate gradient (AMGPCG) solver [Zhang 2015].
(7) **Update liquid particles from grid.** We update each particle's velocity from the MAC grid via APIC [Jiang et al. 2015].
(8) **Update particle deformation info.** The deformation gradient, left Cauchy-Green strain, and volume change are updated through MLS-MPM [Hu et al. 2018].
(9) **Update positions for particles and strands.** Positions are updated according to the velocities for liquid particles and strand vertices.
(10) **Compute plasticity for bulk liquid.** The plastic flow of bulk liquid is computed from the deformation gradient, where excess elastic strain is converted to plastic strain.
(11) **Compute plasticity for surface flow.** The strain in the surface flow is updated by (3), where excess elastic strain is converted to plastic strain.
(12) **Compute plastic recovery.** The plasticity history is relaxed to account for the strengthening of bonds between bulk materials [Yue et al. 2015].

S13 SURFACE RECONSTRUCTION

When generating the liquid particles, we sample 64 particles in each cell occupied by the liquid, where we precompute a level set to cull the particles sampled outside the generator. This amount of particles provides a smoother liquid surface during the reconstruction. We use the VDB [Museth 2013] surface operators (SOPs) in Houdini [SideFX 2019] to perform the reconstruction. For each frame, we use a *VDB from particle liquid* SOP to convert the particles into a level set. To avoid incorrect holes or instability, we turn off the *rebuild* option and use a *Primitive* SOP to categorize the resulting VDB as a level set, which is followed by a *VDB renormalize* SOP to make sure the gradient of the level set is normalized. In the *VDB from particle liquid* SOP, we set the *particle separation* to be $0.5\Delta x$ where Δx is the cell size for simulation, and the *voxel size* (for reconstruction) is set to be 0.25, which means the resolution of the reconstruction grid is 8× higher than the simulation grid. We then perform a dilation-smooth-erosion operation [Museth 2014] to smooth the level set and use a *Convert VDB* node to generate a polygonal surface mesh, where the smoothing method is set to *Mean Curvature Flow* so that the volume is better preserved during smoothing. To better match the volume of the region enclosed by the reconstructed surface to the volume recorded on the particles, we enlarge the distance of erosion by $1.5\Delta x$.

For the surface flow on the strands, we first use a *PolyCut* SOP to remove the strand vertices that have zero flow height on a vertex itself and its neighborhood. Then we use a *Polywire* SOP to convert the height field on the remaining polylines into polygonal meshes.

We merge these two sets of polygons, and use a *VDB from polygons* SOP to convert the merged polygons back into a VDB with much higher resolution, with the *voxel size* set to 0.03 (cm). Then, we again perform a series of dilation-smooth-erosion operation [Museth 2014] to smooth out the kinks around the connections between the bulk liquid and the surface flow, which in addition, also creates the liquid bridge between the flow on strands. Finally, we convert the level set back into polygons for rendering with a *convert VDB* SOP.

S14 PARAMETERS

The physical parameters used in this paper are taken from various sources in the literature [Ardakani et al. 2014; Bochkarev et al. 2009; Kelessidis et al. 2006; Nagasawa et al. 2019; Yue et al. 2015]. These parameters are given in the following table, where the water and tetrachloroethylene are *incompressible, Newtonian* liquids, the drilling mud, acrylic paint and oyster sauce are *incompressible, shear-thinning* liquids, the milk cream and shaving cream are *compressible, shear-thinning* liquids, and the milk chocolate is a *compressible, (almost) Bingham* liquid.

Materials	ρ_f (g/cm^3)	κ ($dyne/cm^2$)	μ ($dyne/cm^2$)	τ_Y ($dyne/cm^2$)	η ($Ba \cdot s^n$)	n (unitless)
water	1.0	2.0e10	0	0	8.9e-3	1.0
tetrachloroethylene	1.622	3.1e10	0	0	8.9e-3	1.0
drilling mud	1.22	2.0e10	1.0e3	16.813	6.496	0.5173
acrylic paint	0.95	1.35e9	4.0e3	9.6	173.56	0.3162
milk cream	0.275	1.09e6	1.6e4	1.2e3	50.0	0.27
shaving cream	0.2	1.09e6	2.9e3	3.19e2	2.72e2	0.22
oyster sauce	1.207	2e10	4.0e3	26.5	16.1	0.62
milk chocolate	0.95	4.28e6	4.0e3	3.0e2	28.0	0.98

S15 IMPORTANCE OF COMPONENTS

While we simulated all the examples in this paper, we have gained some empirical knowledge about the importance of components to visual looks, whereby we color the components accordingly. We hope that this empirical knowledge will help potential readers to reproduce our framework more easily. In Table S1 we list all the components that need to be implemented and color them according to their importance.

Phases	Components
Bulk liquid	Advection
	Pressure
	Merge/Split/Relax Particles
	Shear Stress
	Plastic Flow
	Varying Compressibility
Hairs	Nonlinear Newton Solve
	Contact and Cohesion
Surface Flow	Friction
	Advection
	Shear Stress
	Plastic Flow
Coupling	Hair Momentum from Flow
	Liquid Capturing
	Drag Force
	Boundary Conditions
	Liquid Dripping
	Varying Vol. Frac.

Table S1. **Impact of different components on the visual look.** Component is crucial, empirically, for: ■ all kinds of scenarios; ■ shear-dependent liquid; ■ liquid that has significant inertia or volume fraction with large spatial variance; ■ secondary effect in most cases.

REFERENCES

T B Anderson and Roy Jackson. 1967. Fluid mechanical description of fluidized beds. Equations of motion. *Industrial & Engineering Chemistry Fundamentals* 6, 4 (1967), 527–539.

Ryoichi Ando, Nils Thurey, and Reiji Tsuruno. 2012. Preserving fluid sheets with adaptively sampled anisotropic particles. *IEEE Transactions on Visualization and Computer Graphics* 18, 8 (2012), 1202–1214.

Hesam Anvari Ardakani, Evan Mitsoulis, and Savvas G Hatzikiriakos. 2014. Capillary flow of milk chocolate. *Journal of Non-Newtonian Fluid Mechanics* 210 (2014), 56–65.

DD Atapattu, RP Chhabra, and PHT Uhlherr. 1995. Creeping sphere motion in Herschel-Bulkley fluids: flow field and drag. *Journal of Non-Newtonian Fluid Mechanics* 59, 2-3 (1995), 245–265.

Adam W Bargteil, Chris Wojtan, Jessica K Hodgins, and Greg Turk. 2007. A finite element method for animating large viscoplastic flow. *ACM Transactions on Graphics (TOG)* 26, 3 (2007), 16.

Miklós Bergou, Basile Audoly, Etienne Vouga, Max Wardetzky, and Eitan Grinspun. 2010. Discrete viscous threads. *ACM Transactions on Graphics (TOG)* 29, 4 (2010), 116.

Miklós Bergou, Max Wardetzky, Stephen Robinson, Basile Audoly, and Eitan Grinspun. 2008. Discrete Elastic Rods. *ACM Transactions on Graphics (TOG)* 27, 3 (aug 2008), 63:1–63:12.

AA Bochkarev, PI Geshev, VI Polyakova, and NI Yavorskii. 2009. Formal rheological model of acrylic waterborne paints. *Theoretical Foundations of Chemical Engineering* 43, 1 (2009), 100–107.

Javier Bonet and Richard D Wood. 1997. *Nonlinear continuum mechanics for finite element analysis.* Cambridge university press.

Percy Williams Bridgman. 1949a. Linear Compressions to 30,000 kg/cm^2, including Relatively Incompressible Substances. *Proceedings of the American Academy of Arts and Sciences* 77, 6 (1949), 189–234.

Percy Williams Bridgman. 1949b. *The physics of high pressure.* London: Bells and Sons.

Philippe Coussot. 2017. *Mudflow rheology and dynamics.* Routledge.

Gilles Daviet, Florence Bertails-Descoubes, and Laurence Boissieux. 2011. A hybrid iterative solver for robustly capturing coulomb friction in hair dynamics. *ACM Transactions on Graphics (TOG)* 30, 6 (2011), 139.

G De Saxcé and Z-Q Feng. 1998. The bipotential method: a constructive approach to design the complete contact law with friction and improved numerical algorithms. *Mathematical and Computer Modelling* 28, 4-8 (1998), 225–245.

R Di Felice. 1994. The voidage function for fluid-particle interaction systems. *International Journal of Multiphase Flow* 20, 1 (1994), 153–159.

Yun (Raymond) Fei, Christopher Batty, Eitan Grinspun, and Changxi Zheng. 2018. A multi-scale model for simulating liquid-fabric interactions. *ACM Transactions on Graphics (TOG)* 37, 4 (2018), 51.

Yun (Raymond) Fei, Henrique Teles Maia, Christopher Batty, Changxi Zheng, and Eitan Grinspun. 2017. A Multi-scale Model for Simulating Liquid-hair Interactions. *ACM Transactions on Graphics (TOG)* 36, 4, Article 56 (July 2017), 17 pages.

Masao Fukushima, Zhi-Quan Luo, and Paul Tseng. 2002. Smoothing functions for second-order-cone complementarity problems. *SIAM Journal on optimization* 12, 2 (2002), 436–460.

Ming Gao, Andre Pradhana, Xuchen Han, Qi Guo, Grant Kot, Eftychios Sifakis, and Chenfanfu Jiang. 2018. Animating fluid sediment mixture in particle-laden flows. *ACM Transactions on Graphics (TOG)* 37, 4 (2018), 149.

Winslow H Herschel and Ronald Bulkley. 1926. Konsistenzmessungen von gummi-benzollösungen. *Colloid & Polymer Science* 39, 4 (1926), 291–300.

Yuanming Hu, Yu Fang, Ziheng Ge, Ziyin Qu, Yixin Zhu, Andre Pradhana, and Chenfanfu Jiang. 2018. A moving least squares material point method with displacement discontinuity and two-way rigid body coupling. *ACM Transactions on Graphics (TOG)* 37, 4 (2018), 150.

Geoffrey Irving, Joseph Teran, and Ronald Fedkiw. 2004. Invertible finite elements for robust simulation of large deformation. In *Proceedings of the 2004 ACM SIGGRAPH/Eurographics symposium on Computer animation.* Eurographics Association, 131–140.

M Khalid Jawed, Alyssa Novelia, and Oliver M O'Reilly. 2018. *A primer on the kinematics of discrete elastic rods.* Springer.

Chenfanfu Jiang, Craig Schroeder, Andrew Selle, Joseph Teran, and Alexey Stomakhin. 2015. The affine particle-in-cell method. *ACM Transactions on Graphics (TOG)* 34, 4 (2015), 51.

Ben Jones, Stephen Ward, Ashok Jallepalli, Joseph Perenia, and Adam W Bargteil. 2014. Deformation embedding for point-based elastoplastic simulation. *ACM Transactions on Graphics (TOG)* 33, 2 (2014), 21.

Jonathan M. Kaldor, Doug L. James, and Steve Marschner. 2010. Efficient Yarn-based Cloth with Adaptive Contact Linearization. *ACM Transactions on Graphics (TOG)* 29, 4, Article 105 (July 2010), 10 pages.

VC Kelessidis, R Maglione, C Tsamantaki, and Y Aspirtakis. 2006. Optimal determination of rheological parameters for Herschel–Bulkley drilling fluids and impact on pressure drop, velocity profiles and penetration rates during drilling. *Journal of Petroleum Science and Engineering* 53, 3-4 (2006), 203–224.

E Mauret and M Renaud. 1997. Transport phenomena in multi-particle systems—II. Proposed new model based on flow around submerged objects for sphere and fiber beds-transition between the capillary and particulate representations. *Chemical Engineering Science* 52, 11 (1997), 1819–1834.

R v Mises. 1913. Mechanik der festen Körper im plastisch-deformablen Zustand. *Nachrichten von der Gesellschaft der Wissenschaften zu Göttingen, Mathematisch-Physikalische Klasse* 1913 (1913), 582–592.

Ken Museth. 2013. VDB: High-resolution sparse volumes with dynamic topology. *ACM Transactions on Graphics (TOG)* 32, 3 (2013), 27.

Ken Museth. 2014. A flexible image processing approach to the surfacing of particle-based fluid animation (invited talk). In *Mathematical Progress in Expressive Image*

Synthesis I. Springer, 81–84.

Kentaro Nagasawa, Takayuki Suzuki, Ryohei Seto, Masato Okada, and Yonghao Yue. 2019. Mixing Sauces: A Viscosity Blending Model for Shear Thinning Fluids. *ACM Transactions on Graphics (TOG)* 38, 4 (2019).

Kaare Brandt Petersen, Michael Syskind Pedersen, et al. 2008. The matrix cookbook. *Technical University of Denmark* 7, 15 (2008), 510.

P Rajitha, RP Chhabra, NE Sabiri, and Jacques Comiti. 2006. Drag on non-spherical particles in power law non-Newtonian media. *International Journal of Mineral Processing* 78, 2 (2006), 110–121.

RS Rivlin. 1948. Large elastic deformations of isotropic materials IV. Further developments of the general theory. *Philosophical Transactions of the Royal Society A* 241, 835 (1948), 379–397.

Yousef Saad. 2003. *Iterative methods for sparse linear systems*. Vol. 82. siam.

SideFX. 2019. SideFX Houdini. https://www.sidefx.com.

Juan C Simo. 1988a. A framework for finite strain elastoplasticity based on maximum plastic dissipation and the multiplicative decomposition: Part I. Continuum formulation. *Computer methods in applied mechanics and engineering* 66, 2 (1988), 199–219.

Juan C Simo. 1988b. A framework for finite strain elastoplasticity based on maximum plastic dissipation and the multiplicative decomposition. Part II: computational aspects. *Computer Methods in Applied Mechanics and Engineering* 68, 1 (1988), 1–31.

Juan C Simo and Thomas JR Hughes. 2006. *Computational inelasticity*. Vol. 7. Springer Science & Business Media.

Alexey Stomakhin, Craig Schroeder, Chenfanfu Jiang, Lawrence Chai, Joseph Teran, and Andrew Selle. 2014. Augmented MPM for phase-change and varied materials. *ACM Transactions on Graphics (TOG)* 33, 4 (2014), 138.

Denis L Weaire and Stefan Hutzler. 2001. *The physics of foams*. Oxford University Press.

Martin Wicke, Daniel Ritchie, Bryan M Klingner, Sebastian Burke, Jonathan R Shewchuk, and James F O'Brien. 2010. Dynamic local remeshing for elastoplastic simulation. *ACM Transactions on graphics (TOG)* 29, 4 (2010), 49.

Rene Winchenbach, Hendrik Hochstetter, and Andreas Kolb. 2017. Infinite continuous adaptivity for incompressible SPH. *ACM Transactions on Graphics (TOG)* 36, 4 (2017), 102.

Yonghao Yue, Breannan Smith, Christopher Batty, Changxi Zheng, and Eitan Grinspun. 2015. Continuum foam: A material point method for shear-dependent flows. *ACM Transactions on Graphics (TOG)* 34, 5 (2015), 160.

Yonghao Yue, Breannan Smith, Peter Yichen Chen, Maytee Chantharayukhonthorn, Ken Kamrin, and Eitan Grinspun. 2018. Hybrid Grains: Adaptive Coupling of Discrete and Continuum Simulations of Granular Media. *ACM Transactions on Graphics (TOG)* 37, 6, Article 283 (Nov. 2018), 19 pages.

Xinxin Zhang. 2015. A TBB Parallelized Liquid Solver Featuring Simple FLIP and AMGPCG Pressure Solver. https://github.com/zhxx1987/tbb_liquid_amgpcg.